Research Square

Preprints are preliminary reports that have not undergone peer review.
They should not be considered conclusive, used to inform clinical practice,
or referenced by the media as validated information.

A Human iPSC-Based Lung Organoid with Stromal and Macrophage Components for Pulmonary Fibrosis Modelling and Pharmacological Response Assessment

Huan Zou
Zhujiang Hospital，Southern Medical University
Ze-Xin Chen
Accurate International Biotechnology Limited Company, Guangzhou
Yu Zhu
Accurate International Biotechnology Limited Company, Guangzhou
Suo-Ri-Ya Meng
Accurate International Biotechnology Limited Company, Guangzhou
Dian-Qi Wu
Accurate International Biotechnology Limited Company, Guangzhou
Yi Gao
gaoyi6146@163.com

Zhujiang Hospital，Southern Medical University

Research Article

Keywords: Lung organoids, Fibroblasts, Macrophages, Human induced pluripotent stem cells (hiPSCs), Pulmonary fibrosis (PF), Pharmacological assessment, Drug-associated pulmonary responses

Posted Date: November 2nd, 2026

DOI: https://doi.org/10.21203/rs.3.rs-11386731/v1

License: This work is licensed under a Creative Commons Attribution 4.0 International License.
Read Full License

Additional Declarations: No competing interests reported.

A Human iPSC-Based Lung Organoid with Stromal and Macrophage Components for Pulmonary Fibrosis Modelling and Pharmacological Response Assessment

Huan Zou[#*1], Ze-Xin Chen[2,3], Yu Zhu[2,3], Suo-Ri-Ya Meng[2,3], Dian-Qi Wu[2,3], Yi Gao[*1]

1. Department of Hepatobiliary Surgery II, GuangDong Engineering Technology Research Center of Artificial Organ and Tissue Engineering, Institute of Regenerative Medicine, General Surgery Center, Zhujiang Hospital; State Key Laboratory of Multi-organ Injury Prevention and Treatment; Guangdong Provincial Key Laboratory for Prevention and Control of Major Liver Diseases, Southern Medical University, Guangzhou, China.
2. Guangdong Research Center of Organoid Engineering and Technology, Guangzhou 510530, China
3. Accurate International Biotechnology Limited Company, Guangzhou, Guangdong, China

*Correspondence to:
Yi Gao. Ph.D. E-mail: gaoyi6146@163.com;
Huan Zou. Ph.D. Email: zouhuan_1994@163.com.

Abstract

Background: Pulmonary fibrosis (PF) involves epithelial, stromal, and immune responses that are incompletely represented in conventional culture systems. We therefore sought to engineer a reconstructable human multicellular lung organoid model for PF modelling and pharmacological response assessment.
Methods: The hiLOFM model was assembled by combining human induced pluripotent stem cell-derived lung organoids (hiLOs), human fibroblasts (HFs), and hiPSC-derived macrophages (hiMacs) at a defined starting ratio of 1:2:0.5. Whole-culture responses were evaluated after sequential LPS/TGF-β1 induction, bleomycin (BLM) exposure, and sequential BLM/TGF-β1 treatment. Responses to pirfenidone, nintedanib, and DS-8201 were assessed using morphological, molecular, immunostaining, and cytokine analyses.
Results: The hiLOFM model exhibited increased myofibroblast activation, extracellular matrix deposition, and inflammatory signalling following co-culture with HFs and LPS/TGF-β1-based induction. Macrophage incorporation differentially modulated selected fibrosis- and inflammation-associated readouts. Passaged hiLOs retained selected pulmonary lineage-associated populations and marker expression, and remained capable of supporting reconstruction of the fibrosis-responsive multicellular model. Beyond the LPS/TGF-β1-based condition, BLM alone or combined with TGF-β1 elicited distinct epithelial, fibrotic, and inflammatory responses. For therapeutic

assessment, pirfenidone and nintedanib, alone or in combination, attenuated selected induced responses. For drug-associated pulmonary response assessment, DS-8201 produced concentration- and endpoint-dependent alterations in epithelial, inflammatory, and profibrotic readouts.
Conclusions: We established a repeatedly reconstructable human multicellular model combining expandable hiPSC-derived lung organoids with defined stromal and macrophage inputs. The platform detected responses to multiple fibrogenic and pharmacological conditions, supporting its application in PF modelling, therapeutic-response assessment, and early detection of drug-associated pulmonary response signals.
Keywords: Lung organoids, Fibroblasts, Macrophages, Human induced pluripotent stem cells (hiPSCs), Pulmonary fibrosis (PF), Pharmacological assessment, Drug-associated pulmonary responses

Introduction

Idiopathic pulmonary fibrosis (IPF) is a progressive interstitial lung disease associated with substantial morbidity and mortality; the two approved antifibrotic agents, pirfenidone and nintedanib, only slow the annual rate of lung function decline by approximately 50% in IPF patients, with about 30% discontinuing treatment due to severe side effects[1]. Development of new therapies is limited in part by the availability of preclinical models that combine human cellular relevance with experimentally accessible readouts.

Animal models, particularly bleomycin-induced pulmonary fibrosis in mice, have been instrumental in elucidating fundamental mechanisms of fibrosis. However, they incompletely represent the chronic progression and cellular heterogeneity of human PF, and species differences can limit translation[2,3]. Conversely, two-dimensional cultures and early lung organoid systems provide experimentally tractable human models but often contain only a subset of the epithelial, stromal, and immune components present in fibrotic lung tissue[4-9]. Multicellular human systems may therefore complement existing models in preliminary pharmacological assessment.

In fibrotic lung tissue, injured epithelial cells, activated fibroblasts, and immune cells contribute to a complex microenvironment[10-13]. Macrophages in particular have been associated with fibroblast activation and disease progression[12,14-16]. Although human pluripotent stem cell (hiPSC)-derived lung organoids have increased the cellular relevance of in vitro lung models7,17,18, many reported systems incorporate either fibroblasts or macrophages rather than both [19-22]. A model containing epithelial, stromal, and macrophage components could therefore support investigation of whole-culture responses under experimentally induced fibrotic conditions.

Here, we developed a human iPSC-based lung organoid–fibroblast–macrophage tri-culture model (hiLOFM) integrating expandable hiPSC-derived lung organoids, human fibroblasts, and hiPSC-derived macrophages. We evaluated macrophage-associated effects, model reconstruction using passaged hiLOs, and fibrotic and inflammatory responses to LPS/TGF-β1 and bleomycin-based induction. We further assessed antifibrotic responses to pirfenidone and nintedanib and drug-associated pulmonary responses to DS-8201, examining the model's utility for PF modelling and early-stage pharmacological assessment.

Materials and Methods

Animals

Male C57BL/6 mice (4-6 weeks old) were purchased from Jennio Biotech Company (GuangZhou, China). A total of five mice were used in our study. All animal experiments involved in this study were approved by the Ethics Committee of Zhujiang Hospital of Southern Medical University. All subsequent experiments were performed *in vitro* using established lung organoids. The work has been reported in line with the ARRIVE guidelines 2.0.

Establishment and culture of mouse lung organoids

Mouse lung organoids (mLOs) (Figure S1 and Figure S2) were derived from mouse lung tissues, in which endogenous epithelial stem/progenitor cells were cultured to form self-assembled lung organoids in 3D culture conditions and generated as described previously[23]. Briefly, Lung tissues from C57BL/6 mice after euthanasia with carbon dioxide were used exclusively for immediate lung organoids harvest. No survival surgery or prolonged anesthesia was involved in this study. Upon receipt, the tissues were minced and subjected to enzymatic digestion within a solution comprising dispase II (Roche; #04942078001), DNase I (MilliporeSigma, #10104159001) and collagenase III (Gibco, #17101−015) at 37°C for 2 h. Post- digestion, the supernatant was filtered with 40 μm cell strainer (JET BIOFIL, #CSS013040) and centrifugated at 200 g for 5 min, seeded at a density of 1×10^6 cells/mL. There were two methods for mLOs culturing, maintained in Matrigel: The pellets were resuspended in culture media and mixed with Matrigel (Corning, #356231) at a ratio of 1:1.5 (v:v), subsequently, transferred into a 6 well plate at dropwise. Finally, these droplets were allowed to solidify in a 37°C 5% CO2 incubator for 10 min and culture medium was added and refreshed every 2 − 3 days; Suspension culture: The pellets were resuspended in culture media with 10μM Y27632 onto low-attachment 6-well plates (Corning), culture medium was changed after 48 h and refreshed every 2–3 days. Male C57BL/6 mice aged 4–6 weeks were procured from Jennio Biotech Company (GuangZhou, China). A total of five mice were used in our study. All animal experiments conducted adhered to the Ethics Committee of Zhujiang Hospital of Southern Medical University (LAEC-2022-080) and were in in compliance with relevant guidelines of the Chinese government and regulations for the care and use of experimental animals. Mouse lung tissues used for ex vivo organoid establishment were collected between July 2022 and March 2023.

Establishment and culture of primary human lung organoids

Human lung organoids (hLOs) (Fig. 1) were generated from surgically resected lung tissues of lung cancer patients. Human lung cancer tissues were obtained with informed written consent and approval by the Institute of Research Ethics Committee of Guangdong Provincial People's Hospital, Guangdong Academy of Medical Sciences (Ethics project number: S2024-765-02), following both national and local laws. Primary human peri-tumor lung tissues used for organoid establishment were collected between May 2024 and February 2025. Briefly, endogenous epithelial stem/progenitor cells were isolated from the tissues minced by scissors to 1-2mm^3, and dissociated with a solution comprising dispase II (Roche; #04942078001), DNase I (MilliporeSigma, #10104159001) and collagenase III (Gibco, #17101–015) at 37°C for 2-4 h. Post- digestion, the supernatant was filtered with 70 μm cell strainer (JET BIOFIL) and centrifugated at 200 g for 5 min, seeded at a density

of 1×10⁶ cells/mL. There were two methods for hLOs culturing, maintained in Matrigel: The pellets were resuspended in culture media and mixed with Matrigel (Corning, #356231) at a ratio of 1:1.5 (v:v), subsequently, transferred into a 6 well plate at dropwise. Finally, these droplets were allowed to solidify in a 37°C 5% CO2 incubator for 10 min and culture medium was added and refreshed every 2–3 days; Suspension culture: The pellets were resuspended in culture media with 10μM Y27632 onto low-attachment 6-well plates (Corning), culture medium was changed after 48 h and refreshed every 2–3 days.

Cell cultures

GFP-hiPSCs (purchased from Beijing Cellapy Biotechnology, Cat. CA4020106) were maintained on Mratrigel (1:100; Corning)-coated plates in mTeSR1 (Stem Cell Technologies). Medium was changed every day, and cells were passaged onto fresh Matrigel-coated plates when cells reach 80% confluence using Gentle Cell Dissociation (Stem Cell Technologies). Fibroblasts (HF and MEF) were isolation from the lung tissues of lung cancer human and C57BL/6 mice, after minced - enzymatic digestion - centrifugation, the cell pellets were resuspended in High Glucose DMEM (Gibco) with 10% fetal bovine serum (FBS, Gibco), 1X Glutamax (Gibco), 1X NEAA (Gibco) and cultured under 37℃, 5% CO2. The next day, fresh 10% FBS-DMEM medium was changed to remove non-adherent cells, and then refresh medium every 3 days, cells were passaged when they become confluent using Trypsin-EDTA (0.25%, Gibco) for 3 minutes, and passaged for 1:3. We recommend to use the primary HF/MEF for the fibrosis organoids model within 4 passages.

Induction of lung organoids from hiPSCs

hiPSC-derived lung organoids (hiLOs) (Fig. 3) were induced and differentiated from human induced pluripotent stem cells (hiPSCs) via a stepwise differentiation protocol toward lung epithelial stem/progenitor cell lineages. Briefly, hiPSCs were maintained in an undifferentiated state at 37℃, 5% CO2 until cells reached about 90% confluence, then cell were treated with Accutase and plated onto low attachment 6-well plates seeded at a density of 1×10⁶ cells/mL in endoderm induction medium of DMEM/F12 (3:1) (Life Technologies) supplemented with 5% knockout serum (Life Technologies), 1X B27, 1% Glutamax,1% NEAA at 37 °C in a 5% CO2 environment, containing 10 μM Y-27632, 1 μM Chir99021, 100 ng/mL human Activin A, for 5-6 days, change the medium every day. The endoderm bodies were switched to anterior foregut endoderm induction medium of DMEM/F12 supplemented with 1X B27, 1% Glutamax, 50 μg/ml ascorbic acid, 10 μM SB-431542 and 5 μM Dorsomorphin for 3 days, change the medium every day. For early stage lung progenitor cells induction, the cell spheres were switched to 3 days of 3 μM Chir99021, 500 nM RA and 20 ng/mL BMP4 treatment. Then cells were switched to lung field progenitor cells induction medium of 3 μM Chir99021, 10 ng/mL FGF10, 10 ng/mL KGF and 20 μM DAPT for 7-14 days. For further maturation, the medium changed with 50 nM Dexamethasone, 100 μM 8-BR-CAMP, 10 ng/mL KGF and 100 μM IBMX.

Induction of macrophages from hiPSCs

hiPSCs were dissociated with Accutase to single cell and then seeded at a density of 1×10⁶ cells/mL and aggregated into embryoid bodies (EBs) by centrifugation on ultra-low attachment 6-well plates in mTeSR1 with 10μM Y-27632 for 48-72 h. For hematopoietic specification, cells were treated with

APEL2 medium supplemented with 20 ng/mL VEGF, 20 ng/mL BMP4 and 5 ng/mL bFGF for 48 h, and supplemented with 50 ng/mL VEGF, 10 ng/mL BMP4, 5 ng/mL bFGF and 50 ng/mL SCF for 3 days. For myeloid lineage differentiation, cells were switched into X-VIVO15 medium with 100 μM 2-mercaptoethanol, 100X glutamax, 100X NEAA, 5% knockout serum, 50 ng/mL VEGF, 10 ng/mL bFGF, 50 ng/mL SCF, 20 ng/mL IL-3, 10 ng/mL IL-6 and 50 ng/mL GM-CSF, 48 h later, plate 40-50 EBs onto 1 well of 6-well plate pre-coated with Matrigel Matrix in medium for attachment. Cells were maintained for 10–15 days, and changed medium every 2-3 days, floating cells from the wells were collected and replated onto new empty Matrigel plates. For macrophages induction, cells were maintained in RPMI 1640 medium with 10% FBS contain 50 ng/mL GM-CSF.

Self-organization of the LOF and LOFM

To provide standardized starting cellular inputs, HFs and hiMacs were added at defined cell-number ratios during each model reconstruction. Based on preliminary tests and relevant literature[4,18], this ratio was selected because it yielded the best combination of co-culture stability, cell viability, and fibrotic phenotype induction. The total starting cellular input was fixed at 5 x 10^5 cells per reconstructed culture. For the LOF two-component system, LO-derived cells and fibroblasts were combined at a cell-number ratio of 1:2; For the LOFM tri-culture system, LO-derived cells, fibroblasts, and hiPSC-derived macrophages (hiMacs) were combined at a cell-number ratio of 1:2:0.5. The cellular components were co-cultured in LO medium in 1.5-mL microcentrifuge tubes for 3–6 days to facilitate self-aggregation. LOFM cultures were additionally maintained with 50 ng/mL GM-CSF. The resulting aggregates were subsequently transferred to 24-well ultra-low-attachment plates for fibrosis induction and pharmacological experiments. Within each model configuration, untreated, fibrosis-induced, and drug-treated groups were established using identical total cell inputs and starting cell ratios. The same standardized assembly procedure was applied across experimental batches and to models reconstructed using passaged hiLOs. All fibrosis-related co-culture experiments were conducted under suspension conditions, providing a matrix-free format that facilitated multicellular aggregation and experimental handling.

RNA extraction

Five to ten organoids per biological replicate were washed three times with PBS and lysed in 50 μL TRIzol reagent (Life Technologies) using a tissue-grinding pestle. An additional 450 μL TRIzol was then added, and samples were incubated for 10 min at room temperature. RNA was then extracted according to the TRIzol method.

Real-time quantitative PCR (qPCR)

cDNA synthesis was performed using 500 ng–1 μg of total RNA and the HifairTM II 1st Strand cDNA Synthesis supermix (YEASEN) enzyme according to the manufacturer's protocol. qPCR reactions were performed using SYBR Green master mix (TAKARA) on a Bio-Rad 384-well machine using the following reaction protocol: 1) 95°C for 30s, 2) 95 °C for 5s, 3)60 °C for 34s, 4) go to 2, 40 cycles, 5) 95°C for 15s, 6) 60 °C for 1min,7) 95°C for 15s. Quantification was performed in Microsoft Excel by calculating the ΔCt value using GAPDH as a reference gene. Relative expression was calculated using the $2^{-\Delta\Delta Ct}$ method after normalization to GAPDH. qPCR measurements were performed in three technical replicates. Each experimental condition included

three biological replicates, defined as independently reconstructed co-culture experiments generated from three independent hiPSC differentiation batches. Technical replicate values were averaged to obtain one value for each biological replicate before statistical analysis. Statistical analyses were performed using GraphPad Prism as specified in the Statistical Analysis section. The error bars denote the mean ± SEM. Variance between groups was assessed using an F-test where applicable. qPCR was performed using the primers listed in Table S1.

Immunofluorescence staining

Organoids were embedded in Matrigel and culture for 24-48 h, then fixed in 4% paraformaldehyde for 30min, incubate in 0.1% Triton-X 100 for 10min, and pre-blocked with 5% goat serum (Vector, IL, USA) in Tris-buffered saline (Welgene) for 1h at room temperature (RT) and incubated with primary antibody at 4°C overnight. After washing with PBS, the sections were incubated with secondary antibody for 1h at RT. Primary antibodies used for immunostaining included antibodies against α-SMA, AQP-5, TTF-1, SP-C, SP-B, Keratin-5, P63, MUC5AC, FOXJ1, CD68, CD45, CD163 (Abcam) which are listed in Table S2. The secondary antibodies (Thermo Fisher Scientific, Waltham, MA, USA) used included Alexa Fluor 488 goat anti-rabbit IgG, Alexa Fluor 594 goat anti-mouse IgG, and Alexa Fluor 594 goat anti-rat IgG. Images were acquired on an OLYMPUS IX73 microscope (Olympus, Tokyo, Japan). For immunofluorescence analysis, hiLOs were collected from three independent hiPSC differentiation experiments. For each differentiation batch, three to five organoids were randomly selected, fixed, and processed in parallel for immunostaining.

IHC

Organoids were washed with D-PBS (JET BIOFIL, Guangzhou, China), fixed with 4% paraformaldehyde (Boster, Wuhan, China) for 30 min, and embedded in paraffin. Paraffin sections (5 μm thick) were deparaffinized in xylene and hydrated in a graded ethanol series. The samples were then stained with H&E, α-SMA, Fibronectin, Collagen I staining kit (Abcam) according to the manufacturer's protocol.

ELISA

IL-1β concentrations in LOFM culture supernatants were measured using Human IL-1 beta ELISA kit (Abcam #ab214025) according to the manufacturer's instructions. The cell supernatant of LOFM organoids after centrifugation for 10 min at 2000×g was collected for protein concentration determination. Then, 50 μL of samples were added to each well with 50 μL Antibody Cocktail. After incubation at room temperature for 2 h, these samples were washed four times with 1× Wash Buffer BT. Then, each well was added with 100 μL TMB Development Solution and incubated for 10 min in dark, followed by washes and addition of 100 μL stop solution. The reaction plates were read using a microplate reader (Thermo-Fisher Scientific) at 450 nm.

Drug and Cytokine Treatment

For pharmacological and stimulatory experiments, organoids were treated with the concentrations specified for each experiment. Reconstructed cultures were initially exposed to LPS for 24–48 h, followed by TGF-β1 treatment for an additional 72–96 h. For bleomycin-based induction, cultures were first exposed to bleomycin at the indicated concentration for 24–48 h. Where combined TGF-

β1/bleomycin stimulation was examined, bleomycin exposure was followed by TGF-β1 treatment for an additional 72–96 h. After completion of fibrosis induction, cultures were treated for 72 h with nintedanib, pirfenidone, or their combination to assess treatment-associated antifibrotic responses. For assessment of DS-8201-associated responses, fibrosis-induced cultures were subsequently exposed to DS-8201 for 72 h. TGF-β1, LPS and bleomycin were dissolved in PBS, and the volume of PBS added to the culture medium did not exceed 0.1% (v/v). Nintedanib and pirfenidone were dissolved in DMSO, with a final concentration of 0.1% (v/v) DMSO in the culture medium. DS-8201 was dissolved in PBS. All treatments were maintained for the indicated duration. Naïve organoids (cultured without any stimulation or drug treatment) served as the baseline negative controls.

Statistical Analysis

All quantitative data are presented as the mean ± standard error of the mean (SEM). Each experiment was independently repeated at least three times (biological replicates, n ≥ 3), biological replicates represented independently differentiated and reconstructed co-culture experiments. Technical replicates were averaged and were not treated as independent observations in the statistical analysis. Statistical comparisons between two groups were performed using two-tailed unpaired Student's t-test. For comparisons among multiple groups, one-way analysis of variance (ANOVA) followed by Tukey's post hoc test. A p-value < 0.05 was considered statistically significant.

Results

Mouse Lung Organoids as a Technical Pilot for Fibrosis-Associated Modeling

Before applying the culture strategy to human cells, we generated mLOs from dissociated C57BL/6 lung tissue as a technical pilot. Immunofluorescence (IF) detected markers associated with epithelial (EPCAM), lung epithelial (TTF1), alveolar type I (AQP5), goblet (MUC5AC), and basal (P63) phenotypes (Fig. S1A). Organoids were maintained in Matrigel or suspension culture, and could be passaged and recovered after cryopreservation (Fig. S2A, Fig. S1B). Morphological examination revealed typical organoid structures, including both cystic and solid morphologies (Fig. S2A). Fibroblasts were added to the mLO cultures to examine whether a stromal component altered fibrosis-associated responses. The fibroblast panel included mouse embryonic fibroblasts, HFL-1 cells, and two human lung tissue-derived fibroblast preparations (Fig. S2B). Co-culture of MEF with mLOs (mLOF) under LPS (1 μg/mL) and sustained TGF-β1 stimulation (25 ng/mL, 96 h) induced morphological restructuring, characterized by a shift from cystic to compact solid spheroids (Fig. S2C, Fig. S3A). Histological analysis confirmed marked stromal expansion (Fig. S2D), and immunohistochemical (IHC) analysis revealed elevated expression of core fibrotic mediators including fibronectin and α-smooth muscle actin (α-SMA). Consistent with these findings, RT-qPCR revealed concomitant upregulation of α-SMA and collagen I (Fig. S2D-E). LPS/TGF-β1 exposure altered these markers in mLO monocultures, whereas cultures containing fibroblasts generally showed higher fibrosis-associated readouts (Fig. S2C-E, Fig. S3B). These whole-culture comparisons supported use of the organoid–fibroblast co-culture in subsequent experiments and demonstrated its ability to capture

integrated epithelial–stromal responses under fibrotic conditions.

We next examined response to the approved antifibrotic agents nintedanib and pirfenidone. Drug treatment was associated with a partial shift toward cystic morphology in previously solid organoids (Fig. S2F, Fig. S3C). This structural change was accompanied by reduced α-SMA expression in treated groups compared to untreated controls (Fig. S2F). RT-qPCR showed downregulation of the fibrotic markers (α-SMA, Collagen I, and MMP2) after drug exposure (Fig. S2G, Fig. S3D). Nintedanib showed more pronounced suppression of these markers than pirfenidone (Fig. S2G). These results provided technical support for evaluating pharmacological responses in the human organoid systems.

Establishment of Fibrosis-Associated and Pharmacological Responses in Primary Human Lung Organoid Co-Cultures

Primary human lung organoids (hLOs) were established from histologically confirmed peri-tumour lung tissue obtained from patients with lung cancer. The cultures formed cystic structures and could be maintained over 3-5 serial passages (Fig. 1A). Immunofluorescence detected markers associated with alveolar type I (AQP5), alveolar type II (TTF-1 and SFTPC), basal (keratin 5 and p63), goblet (MUC5AC), and ciliated (FOXJ1) epithelial phenotypes (Fig. 1B). RT-qPCR further confirmed expression of AQP5, SFTPC, KRT5, and MUC5AC (Fig. 1C). These data demonstrate the presence of multiple pulmonary epithelial-associated markers but do not establish that their relative abundance is preserved across passages or equivalent to normal human lung tissue.

LPS and TGF-β1 exposure was associated with conversion from cystic to more compact structures, increased collagen I, α-SMA, and fibronectin staining, and increased transcription of collagen I, fibronectin, α-SMA, and vimentin (Fig. S4A-B). To incorporate an additional stromal component, hLOs were combined with human fibroblasts and exposed to LPS/TGF-β1. The co-cultures showed higher fibrosis-associated readouts than untreated hLO controls (Fig. 1D-E) and were subsequently used for exploratory pharmacological assessment.

Nintedanib reduced selected markers, including α-SMA and collagen I, whereas other measured markers showed smaller or non-significant changes under the tested conditions; Pirfenidone monotherapy did not significantly reduce the measured transcriptional markers in this experiment (Fig. 1F). Since nintedanib and pirfenidone target distinct signaling pathways involved in fibrotic progression, and combination treatment has been examined clinically[24-26], we also evaluated combined exposure. The combination reduced α-SMA and fibronectin relative to untreated fibrotic co-cultures (Fig. 1G-H). These findings demonstrate that the model captures distinct responses to mono- and combination-treatment regimens, supporting its potential application in the preclinical evaluation of antifibrotic therapeutic strategies.

Macrophage Incorporation Modulates Responses in The Primary Human Lung Organoid Co-culture

To incorporate an immune component, hiPSC-derived macrophages (hiMac) were added to the hLO–fibroblast co-culture. GFP-expressing hiMac were generated by directed differentiation (Fig. 2A) and immunofluorescence detected CD45, CD68, and CD163 (Fig. 2B), consistent with a macrophage-like phenotype under the applied differentiation conditions.

Organoids, fibroblasts, and macrophages were combined at a ratio of 1:2:0.5 selected from preliminary experiments and published work[4,18] . Under LPS/TGF-β1 exposure, the cellular components aggregated into compact spheroids (Suppl. Video 1-4). Macrophage-containing cultures (hLOFM) exhibited greater aggregation, forming spheroids with dimensions substantially exceeding those generated in hLOs or hLOF (Fig. 2C). Because relative cell abundance and spatial organization were not quantified, these observations demonstrate co-aggregation rather than a stable or spatially defined cellular niche.

IF quantification revealed pronounced augmentation of α-SMA expression after LPS and sustained TGF-β1 stimulation, with maximal intensity observed in macrophage-containing systems (hLOFM-F). While hLOF induced expected fibrotic activation, macrophage incorporation was associated with a greater response under the tested conditions (Fig. 2D). Macrophage-containing cultures showed increased fibronectin, α-SMA, and vimentin under fibrotic conditions, whereas collagen I varied across groups (Fig. 2E). Thus, macrophage incorporation modulated multiple fibrosis-associated readouts, supporting an association between macrophage incorporation and the multicellular fibrotic response of the model.

Development of a hiPSC-Based Multicellular Lung Organoid Model

To overcome the limited availability and donor-to-donor variability of primary tissue-derived models (Fig. S4C), we generated hiPSC-derived lung organoids (hiLOs) using a stepwise differentiation protocol. Bright-field imaging documented organoid formation and showed that hiLOs could be serially passaged and recovered after cryopreservation (Fig. 3A–B). Representative morphologies at day 30, day 50, P1, P3, and P4 after cryopreservation further demonstrated preservation of the overall organoid architecture during prolonged culture and expansion (Fig. S5B). These findings demonstrate the practical expandability and recoverability of hiLOs under the tested conditions, potentially reducing the need for repeated de novo differentiation across experimental batches. Immunofluorescence analysis identified cells expressing markers associated with alveolar type I (AQP5), alveolar type II/lung epithelial (TTF1/NKX2.1, SP-B, and SFTPC), basal cells (KRT5), goblet cells (MUC5AC). Small subsets of cells showing CD68 or α-SMA immunoreactivity were also observed within the examined hiLOs (Fig. 3C, Fig. S5A). To assess the retention of selected lineage-associated features during expansion, P3 hiLOs were further characterized by immunofluorescence, AQP5-, SFTPC-, KRT5-, and α-SMA-positive populations remained detectable at P3 (Fig. 3D), and semi-quantitative image analysis estimated their relative abundance within the examined organoids (Fig. S5C–D). RT-qPCR additionally confirmed the expression of NKX2.1, AQP5, SFTPC, and KRT5 at day 30, P1, and P3 (Fig. 3E). Together, these results demonstrate the retention of selected pulmonary lineage-associated features across the examined passages. Spontaneous contractions were also observed (Suppl. Videos 5.1–5.2), suggesting the possible presence of contractile smooth muscle-like cells, although their identity requires further validation.

We next evaluated whether hiLOs could support the construction of a multicellular pulmonary fibrosis model. Freshly differentiated hiLOs were combined with human fibroblasts and hiMac at a fixed starting ratio of 1:2:0.5

to generate the hiLOFM tri-culture. Following LPS/TGF-β1 exposure, macrophage-containing cultures exhibited greater spheroid compaction and structural remodelling than the corresponding macrophage-free cultures (Fig. 4A, Suppl. Video 6-9). Immunostaining and RT-qPCR demonstrated changes in the fibrosis-associated markers α-SMA, fibronectin, and vimentin (Fig. 4B-F), together with increased expression of the fibrosis- and inflammation-associated readouts IL-11 and IL-1β (Fig. 4G, H). These results show that the hiLOFM model develops measurable fibrosis- and inflammation-associated responses at the whole-culture level.

We subsequently examined whether passaged hiLOs retained the capacity to reconstruct the model. P3 hiLOs were incorporated into hiLOF, hiLOM, and hiLOFM configurations and subjected to the same fibrosis-induction procedure. Compared with untreated hiLOF controls, induced hiLOF cultures showed changes in selected fibrosis-associated markers, supporting the responsiveness of the two-component system. Macrophage-containing configurations, particularly induced hiLOFM cultures, displayed stronger changes in selected whole-culture fibrosis and inflammatory readouts, including α-SMA, fibronectin, collagen I, IL-6, IL-1β, and IL-8 (Fig. S6A-C). Together with the retained lineage-marker expression at P3, these findings demonstrate that passaged hiLOs remain capable of supporting reconstruction of the multicellular fibrosis model.

Fibrogenic and pharmacological response assessment using the hiLOFM model

To determine whether the hiLOFM model could respond to different fibrogenic conditions, we evaluated three experimental settings: the original hiLOFM-F induction protocol, BLM exposure alone, and a separate combined treatment consisting of TGF-β1 and BLM. Treatment with BLM at 3 or 10 μg/mL produced concentration- and endpoint-dependent alterations in the fibrosis-associated genes FN1 and COL1A1, the inflammatory readouts IL11 and secreted IL-1β, and the alveolar epithelial lineage-associated genes AQP5 and SFTPC. The combined TGF-β1/BLM treatment produced pronounced changes in selected fibrotic and inflammatory readouts, including FN1, COL1A1, IL11, and IL-1β. These results indicate that the hiLOFM model can register responses to distinct fibrogenic conditions and provide a broader experimental range for pharmacological assessment (Fig. 5A–F). For pharmacological assessment, the nintedanib–pirfenidone combination was evaluated separately in cultures subjected to the original hiLOFM-F induction protocol and in cultures exposed to the TGF-β1/BLM condition. The treatment reduced FN1 expression under both fibrogenic conditions, and reduced IL11 and IL-1β under the TGF-β1/BLM condition. Nintedanib–pirfenidone treatment also increased AQP5 and SFTPC transcript levels, indicating modulation of alveolar epithelial lineage-associated responses. Collectively, these endpoint-specific effects support the potential use of the hiLOFM model as a complementary human in vitro platform for preliminary assessment of antifibrotic treatment responses under different fibrogenic conditions (Fig. 5G–K).

We next investigated whether the model could detect compound-associated pulmonary responses using trastuzumab deruxtecan (DS-8201), an anticancer antibody–drug conjugate associated with a clinically recognized risk of interstitial lung disease and pneumonitis. Across the tested concentration

range of 0.5–50 μg/mL, DS-8201 increased α-SMA fluorescence and induced concentration- and endpoint-dependent changes in ACTA2, FN1, COL1A1, IL11 expression and in secreted IL-1β (Fig. 6A-H). DS-8201 also altered the expression of the alveolar epithelial lineage-associated genes AQP5 and SFTPC, although these responses were non-monotonic across concentrations (Fig. 6J-K). These findings demonstrate that the hiLOFM model can detect DS-8201-associated epithelial, inflammatory, and profibrotic responses across multiple readouts, supporting its exploratory application in the early-stage assessment of drug-associated pulmonary effects.

In summary, the hiLOFM model combines epithelial, fibroblast, and macrophage components and displays selected inflammatory and fibrosis-associated responses after LPS/TGF-β1 exposure. Responses to established antifibrotic agents support its potential use as a complementary human in vitro model for preclinical pharmacological assessment, while its detection of DS-8201-associated responses highlights its potential utility in the early-stage evaluation of drug-associated pulmonary effects (Fig. 7).

Discussion

The aim of this study was to construct a reproducible multicellular human lung organoid model that displays measurable fibrosis- and inflammation-associated phenotypes and supports pharmacological response assessment. Although hiLOs contained small marker-positive populations associated with mesenchymal and macrophage-like phenotypes, defined numbers of human fibroblasts and hiPSC-derived macrophages were externally introduced to provide standardized stromal and macrophage components during model reconstruction. And combining these components also derives from their contributions of epithelial injury, fibroblast activation, and macrophage-associated inflammation to pulmonary fibrosis. However, Previous organoid studies have incorporated fibroblasts or macrophages[4,18-22], and the present model combines both components with hiPSC-derived lung organoids.

Using sequential LPS-induced injury followed by sustained TGF-β1 exposure, the LOFM model exhibited fibrosis-associated responses characterized by myofibroblast activation, ECM deposition and increased pro-inflammatory cytokine secretion. The incorporation of macrophages further enhanced several fibrosis- and inflammation-associated readouts compared with macrophage-free cultures (Fig. 2D-E; Fig. 4B-H), supporting the value of including an immune component when modelling whole-culture fibrosis-associated responses. This finding is consistent with evidence that profibrotic macrophage populations persist in fibrotic lungs and contribute to disease progression through interactions with stromal and epithelial cells[12,16]. Macrophages may influence fibrotic responses through the production of mediators such as TGF-β1, PDGF, and CTGF, as well as through adhesion-associated interactions with fibroblasts[27,28]. Accordingly, incorporating macrophages enables the model to capture fibrosis-associated inflammatory and stromal responses that may be incompletely represented in epithelial–fibroblast co-culture systems.

The model also demonstrated pharmacological responsiveness across both mouse and human organoid systems. In the mouse organoid model, the established antifibrotic agents pirfenidone and nintedanib reduced selected fibrosis-associated markers (Fig. S2F–G). In the human hiLOFM model,

responses to BLM alone and to the combined TGF-β1/BLM condition extended the pharmacological assessment beyond the original LPS/TGF-β1-based fibrosis-induction protocol. In the primary human hLOF co-culture, mono- and combination-treatment groups showed distinct changes in selected fibrosis-associated readouts (Fig. 1F–H). The combination also reduced FN1 expression in both the original hiLOFM-F model and the combined TGF-β1/BLM condition, and reduced IL11 and IL-1β in TGF-β1/BLM condition (Fig. 5G–K). These findings indicate that the model can distinguish endpoint-specific pharmacological responses under different fibrogenic conditions. These experiments were intended to broaden the range of conditions evaluated using the model rather than to define the molecular interactions or pharmacological synergy between agents used in combination.

Nintedanib and pirfenidone act through partially distinct pharmacological mechanisms: inhibition of growth factor receptor signaling by nintedanib and modulation of inflammatory and profibrotic processes by pirfenidone, providing a rationale for investigating their combined use. Clinical studies have explored add-on or combination regimens and have indicated that such treatment may be feasible in selected patients; however, tolerability remains an important consideration, and evidence for additional clinical efficacy remains inconclusive[29,30]. Accordingly, the responses observed in the present organoid models demonstrate the potential of these models to compare mono- and combination-treatment responses in a multicellular pulmonary context. The increases in AQP5 and SFTPC transcripts following antifibrotic treatment further indicate modulation of alveolar epithelial lineage-associated gene expression.

The hiLOFM model also detected responses to trastuzumab deruxtecan (DS-8201), an anticancer antibody–drug conjugate clinically associated with interstitial lung disease and pneumonitis[31,32]. Across the tested concentrations, DS-8201 altered α-SMA, fibrosis-associated genes, inflammatory mediators, and alveolar epithelial lineage-associated markers. These responses were concentration and endpoint dependent and were not uniformly monotonic, suggesting that DS-8201 may produce a combination of epithelial stress, inflammatory signaling, and profibrotic activation within the model. The presence of epithelial, stromal, and macrophage components permits these multiple whole-culture responses to be assessed within the same human cell-based system. Together, these findings demonstrate that the hiLOFM model can detect compound-associated pulmonary responses across multiple cellular and molecular endpoints, supporting its exploratory use as a complementary human in vitro platform for preliminary pharmacological assessment and identification of drug-associated pulmonary response signals.complementary human in vitro platform

Several limitations should be acknowledged. First, this study focused on development and preliminary application of a reproducibly reconstructed whole-culture model. The analyses did not resolve the relative contributions of endogenous marker-positive populations and supplemented HFs or hiMacs, nor did they define cell-specific interactions or the mechanisms underlying combined drug responses. These questions will require lineage-resolved analyses, targeted perturbation, and broader pharmacological validation. And only a single hiPSC line was used to generate hiLOs, confirmation with additional lines will be important to assess the generalizability of these findings.

Second, the current model incorporates M2 macrophages but does not include other immune populations—such as monocytes, neutrophils, or lymphocytes—that may also contribute to fibrotic regulation. Third, while the system captures several cellular and molecular aspects of fibrosis, it does not fully reproduce the architectural complexity or mechanical properties of the human lung. Future studies integrating perfusable vascular networks and additional immune subsets may further improve the physiological relevance of the platform.

Beyond pulmonary fibrosis, this approach may offer a framework for modeling other fibrotic diseases in which microenvironmental crosstalk influences disease progression and treatment response.

This platform aligns with “3Rs” principles by providing an experimentally accessible human cell-based system that could reduce reliance on animal models in early-stage drug screening, and by enabling more detailed investigation of human-specific multicellular interactions within a controlled microenvironment.

Conclusion

We established a repeatedly reconstructable human multicellular model combining expandable hiPSC-derived lung organoids with defined stromal and macrophage inputs. The model generated measurable whole-culture responses to multiple fibrogenic conditions and distinguished responses to established antifibrotic agents and DS-8201 exposure. These findings support its use as a complementary platform for pulmonary fibrosis modelling, therapeutic-response assessment, and early detection of drug-associated pulmonary response signals.

Funding

This study was co-supported by Prevention and Control of Emerging and Major Infectious Diseases-National Science and Technology Major Project (2025ZD01908103), Guangdong S&T Program (2025B1111110001), National Key R&D Program of China (2022YFA1104900).

Author contributions

H.Z. conceived and designed the study, conducted the majority of the experiments, analyzed the data, and wrote the original manuscript draft. D.Q.W. and S.R.Y.M. contributed to the experimental work and data collection. Z.X.C. and Y.Z. participated in the study design and project administration and provided technical support and resources. They also critically reviewed and revised the manuscript. Y.G. supervised the study, acquired funding, and critically reviewed and revised the manuscript. All authors read and approved the final version of the manuscript and agreed to be accountable for their respective contributions.

Declaration of Interest

The authors declare no competing or financial interests.

Acknowledgments

We are grateful to all members of the Y.G laboratory for their insightful discussions and technical assistance. We also thank Accurate International Biotechnology Limited Company for their generous provision of organoid technology support and essential materials.

We thank Yang Li (Professor Yi Gao's laboratory, Southern Medical University), Jia He (Department of Burn Surgery, The First People's Hospital of Foshan, Foshan, Guangdong, China), and Min Li (Guangdong Qianhui Biotechnology Co., Ltd., Guangzhou 510285, China) for their helpful discussions and comments on data presentation during the revision of the manuscript.

During the preparation of this work, the authors used DeepSeek for language polishing, editing, and improving the clarity and fluency of the manuscript text. All scientific content, including data interpretation, conclusions and literature citations, was rigorously reviewed, structured and finalized by the authors. The authors take full responsibility for the entire intellectual content and accuracy of the published work.

Ethics approval and consent to participate

This study did not involve live animal experimentation, interventions, or longitudinal in vivo observation. Tissues were obtained post-euthanasia for in vitro organoid culture only. All animal experiments were approved by the Ethics Committee of Zhujiang Hospital of Southern Medical University (approval number: LAEC-2022-080, approval date: Jul 6, 2022, project name: Mechanisms of mesenchymal stem cells in acute lung injury). The work has been reported in line with the ARRIVE guidelines 2.0.

The human induced pluripotent stem cells (hiPSCs) used in this study were commercially sourced from Beijing Cellapy Biotechnology. The provider has confirmed that informed consent was obtained from all donors and there was initial ethical approval for collection of human cells.

All human experiments were approved by the Institute of Research Ethics Committee of Guangdong Provincial People's Hospital, Guangdong Academy of Medical Sciences (approval number: S2024-765-02, approval date: Mar 6, 2024, project name: Application of human lung cancer organoids and coculture with immune cells), following both national and local laws.

Consent for publication

Not applicable.

Supplementary materials

Table. S1 Primers used in this study

qPCR primers:	qPCR primers:
h-GAPDH-F: 5'-CATGAGAAGTATGACAACAGCCT-3'	h-aSMA-F: 5'- GACGAAGCACAGAGCAAAAG-3'

h-GAPDH-R: 5'-AGTCCTTCCACGATACCAAAGT-3'	h-aSMA-R: 5'- AGTTGGTGATGATGCCATGT-3'
h-AQP5-F: 5'-CGGGCTTTCTTCTACGTGG-3'	h-Fibronectin-F: 5'- TGGATGTTCCTTCCACAGTTCA-3'
h-AQP5-R: 5'-GCTGGAAGGTCAGAATCAGCTC-3'	h-Fibronectin-R: 5'- CATTTGGATTGAGCCCCGGA-3'
h-SFTPC-F: 5'-CCTTCTTATCGTGGTGGTGGT-3'	h-Vimentin-F: 5'-CCAGGCAAAGCAGGAGTC -3'
h-SFTPC-R: 5'- TCTCCGTGTGTTTCTGGCTCAT-3'	h-Vimentin-R: 5'-CGAAGGTGACGAGCCATT -3'
h-Epcam-F: 5'-TGATCCTGACTGCGATGAGAG-3'	h-Collagen I-F: 5'- AAGGGTGAGACAGGCGAACA-3'
h-Epcam-R: 5'- CTTGTCTGTTCTTCTGACCCC-3'	h-Collagen I-R: 5'- GACCCTGGAGGCCAGAGAAG-3'
h-KRT5-F: 5'- TGACCTCCGCAACACCAAG-3'	h-IL-11-F: 5'- CTGTGGGGACATGAACTGTG -3'
h-KRT5-R: 5'- CAGATTGGCGCACTGTTTCTT-3'	h-IL-11-R: 5'- AGGGTCTGGGGAAACTCG -3'
h-MUC5AC-F: 5'- ACCAATGCTCTGTATCCTTCCC -3'	h-IL1b-F: 5'-AGCTACGAATCTCCGACCAC -3'
h-MUC5AC-R: 5'- TGGTGGACGGACAGTCACT -3'	h-IL1b-R: 5'-CGTTATCCCATGTGTCGAAGAA -3'

Table. S2 Primary antibodies used in this study

Antibodies	SOURCE	IDENTIFIER
Anti-alpha smooth muscle Actin antibody	Abcam	ab5694
Anti-Aquaporin 5 antibody	Abcam	ab92320
Anti-TTF1/Nkx2-1 antibody	Abcam	ab76013
Anti-Prosurfactant Protein C antibody	Abcam	ab90716
Anti-Prosurfactant Protein B antibody	Abcam	ab40876
Cytokeratin 5 Antibody	Affinity Bioscience LTD	AF5479
Anti-p63 antibody	Abcam	ab124762
Anti-Mucin 5AC antibody	Abcam	ab229451
Anti-FoxJ1 antibody	Abcam	ab235445
Anti-CD68 antibody	Abcam	ab955
Anti-CD45 antibody	Abcam	ab40763
Anti-CD163 antibody	Abcam	ab182422
Anti-Fibronectin antibody	Abcam	ab2413
Anti-Vimentin antibody	Abcam	ab8978
Anti-Collagen I antibody	Abcam	ab138492

Data Availability

The supplementary videos supporting the findings of this study are openly available in Zenodo at https://doi.org/10.5281/zenodo.21502299. The remaining data that support the findings of this study are available from the corresponding authors, Huan Zou and Yi Gao, upon reasonable request. Requests for access to the data should be directed to Huan Zou (zouhuan_1994@163.com) or Yi Gao (gaoyi6146@163.com)

References

1 Guler, S. A., Lindell, K. O., Swigris, J. & Ryerson, C. J. Medications for Idiopathic Pulmonary Fibrosis: IPF Part 2. *Am J Respir Crit Care Med* **203**, P7-p8 (2021). https://doi.org:10.1164/rccm.2033P7

2 Kong, J. *et al.* Lung organoids, useful tools for investigating epithelial repair after lung injury. *Stem Cell Res Ther* **12**, 95 (2021). https://doi.org:10.1186/s13287-021-02172-5

3 Jenkins, R. G. *et al.* An Official American Thoracic Society Workshop Report: Use of Animal Models for the Preclinical Assessment of Potential Therapies for Pulmonary Fibrosis. *Am J Respir Cell Mol Biol* **56**, 667-679 (2017). https://doi.org:10.1165/rcmb.2017-0096ST

4 Heo, H. R. & Hong, S. H. Generation of macrophage containing alveolar organoids derived from human pluripotent stem cells for pulmonary fibrosis modeling and drug efficacy testing. *Cell Biosci* **11**, 216 (2021). https://doi.org:10.1186/s13578-021-00721-2

5 Wang, D., Haviland, D. L., Burns, A. R., Zsigmond, E. & Wetsel, R. A. A pure population of lung alveolar epithelial type II cells derived from human embryonic stem cells. *Proc Natl Acad Sci U S A* **104**, 4449-4454 (2007). https://doi.org:10.1073/pnas.0700052104

6 Huang, S. X. *et al.* Efficient generation of lung and airway epithelial cells from human pluripotent stem cells. *Nat Biotechnol* **32**, 84-91 (2014). https://doi.org:10.1038/nbt.2754

7 Jacob, A. *et al.* Differentiation of Human Pluripotent Stem Cells into Functional Lung Alveolar Epithelial Cells. *Cell Stem Cell* **21**, 472-488.e410 (2017). https://doi.org:10.1016/j.stem.2017.08.014

8 Jacob, A. *et al.* Derivation of self-renewing lung alveolar epithelial type II cells from human pluripotent stem cells. *Nat Protoc* **14**, 3303-3332 (2019). https://doi.org:10.1038/s41596-019-0220-0

9 McCauley, K. B. *et al.* Efficient Derivation of Functional Human Airway Epithelium from Pluripotent Stem Cells via Temporal Regulation of Wnt Signaling. *Cell Stem Cell* **20**, 844-857.e846 (2017). https://doi.org:10.1016/j.stem.2017.03.001

10 Habermann, A. C. et al. Single-cell RNA sequencing reveals profibrotic roles of distinct epithelial and mesenchymal lineages in pulmonary fibrosis. Science Advances 6, eaba1972 (2020). https://doi.org/10.1126/sciadv.aba1972

11 Adams, T. S. *et al.* Single-cell RNA-seq reveals ectopic and aberrant lung-resident cell populations in idiopathic pulmonary fibrosis. *Sci Adv* **6**, eaba1983 (2020). https://doi.org:10.1126/sciadv.aba1983

12 Misharin, A. V. *et al.* Monocyte-derived alveolar macrophages drive lung fibrosis and persist in the lung over the life span. *J Exp Med* **214**, 2387-2404 (2017). https://doi.org:10.1084/jem.20162152

13 Chanda, D. *et al.* Developmental pathways in the pathogenesis of lung fibrosis. *Mol Aspects Med* **65**, 56-69 (2019). https://doi.org:10.1016/j.mam.2018.08.004

14 Fabre, T. *et al.* Identification of a broadly fibrogenic macrophage subset induced by type 3 inflammation. *Sci Immunol* **8**, eadd8945 (2023). https://doi.org:10.1126/sciimmunol.add8945

15 Unterman, A. *et al.* Single-Cell Profiling Reveals Immune Aberrations in Progressive Idiopathic Pulmonary Fibrosis. *Am J Respir Crit Care Med* **210**, 484-496 (2024). https://doi.org:10.1164/rccm.202306-0979OC

16 Lodyga, M. *et al.* Cadherin-11-mediated adhesion of macrophages to myofibroblasts establishes a profibrotic niche of active TGF-β. *Sci Signal* **12** (2019). https://doi.org:10.1126/scisignal.aao3469

17 Dye, B. R. *et al.* In vitro generation of human pluripotent stem cell derived lung organoids. *Elife* **4** (2015). https://doi.org:10.7554/eLife.05098

18 Suezawa, T. *et al.* Disease modeling of pulmonary fibrosis using human pluripotent stem cell-derived alveolar organoids. *Stem Cell Reports* **16**, 2973-2987 (2021). https://doi.org:10.1016/j.stemcr.2021.10.015

19 Ptasinski, V. *et al.* Modeling fibrotic alveolar transitional cells with pluripotent stem cell-derived alveolar organoids. *Life Sci Alliance* **6** (2023). https://doi.org:10.26508/lsa.202201853

20 Strikoudis, A. *et al.* Modeling of Fibrotic Lung Disease Using 3D Organoids Derived from Human Pluripotent Stem Cells. *Cell Rep* **27**, 3709-3723.e3705 (2019). https://doi.org:10.1016/j.celrep.2019.05.077

21 Wang, H. *et al.* Modeling of lung organoid-based fibrosis for testing the sensitivity of anti-fibrotic drugs. *Stem Cell Res Ther* **16**, 132 (2025). https://doi.org:10.1186/s13287-025-04251-3

22 Xu, Y., Ying, L., Lang, J. K., Hinz, B. & Zhao, R. Modeling mechanical activation of macrophages during pulmonary fibrogenesis for targeted anti-fibrosis therapy. *Sci Adv* **10**, eadj9559 (2024). https://doi.org:10.1126/sciadv.adj9559

23 Yu, Y. *et al.* Molecular distinctions of bronchoalveolar and alveolar organoids under differentiation conditions. *Physiol Rep* **12**, e16057 (2024). https://doi.org:10.14814/phy2.16057

24 Huh, J. Y., Lee, J. H. & Song, J. W. Efficacy and safety of combination therapy with pirfenidone and nintedanib in patients with idiopathic pulmonary fibrosis. *Front Pharmacol* **14**, 1301923 (2023). https://doi.org:10.3389/fphar.2023.1301923

25 Meng, C., Fan, G., Liu, J., Tao, N. & Sun, T. Pirfenidone and nintedanib exert additive antifibrotic effects by the SPP1-AKT pathway in macrophages and fibroblasts. *Biochem Biophys Res Commun* **716**, 150020 (2024). https://doi.org:10.1016/j.bbrc.2024.150020

26 Vancheri, C. *et al.* Nintedanib with Add-on Pirfenidone in Idiopathic Pulmonary Fibrosis. Results of the INJOURNEY Trial. *Am J Respir Crit Care Med* **197**, 356-363 (2018). https://doi.org:10.1164/rccm.201706-1301OC

27 Wynn, T. A. & Vannella, K. M. Macrophages in Tissue Repair, Regeneration, and Fibrosis. *Immunity* **44**, 450-462 (2016). https://doi.org:10.1016/j.immuni.2016.02.015

28 Zhang, Z. Q., Tian, H. T., Liu, H. & Xie, R. The role of macrophage-derived TGF-β1 on SiO(2)-induced pulmonary fibrosis: A review. *Toxicol Ind Health* **37**, 240-250 (2021). https://doi.org:10.1177/0748233721989896

29 Kondoh, Y., Ito, T., Kimura, H., Bao, H. & Kuwana, M. Patient characteristics and pharmacologic treatment patterns in antifibrotic-treated patients with fibrosing interstitial lung diseases: real-world results from a claims database. *BMC Pulm Med* **25**, 253 (2025). https://doi.org:10.1186/s12890-025-03713-x

30 Lee, J. & Song, J. U. Safety and tolerability of combination treatment with pirfenidone and nintedanib in patients with idiopathic pulmonary fibrosis: a systematic review and meta-analysis. *J Thorac Dis* **15**, 5913-5921 (2023). https://doi.org:10.21037/jtd-23-946

31 Ogitani, Y. *et al.* DS-8201a, A Novel HER2-Targeting ADC with a Novel DNA Topoisomerase I Inhibitor, Demonstrates a Promising Antitumor Efficacy with Differentiation from T-DM1. *Clin Cancer Res* **22**, 5097-5108 (2016). https://doi.org:10.1158/1078-0432.Ccr-15-2822

32 Spagnolo, P., Bonniaud, P., Rossi, G., Sverzellati, N. & Cottin, V. Drug-induced interstitial

Figure legend

Figure 1 Primary Human Lung Organoid Co-Cultures Display Fibrosis-Associated and Pharmacological Responses. Human lung organoids (hLOs) were derived from endogenous epithelial stem/progenitor cells isolated from surgically resected lung tissues of lung cancer patients. **A** Bright-field morphology of hLOs derived from human lung tumor specimens. **B** Immunofluorescence (IF) staining validating key pulmonary cell identities in hLOs, the upper panel shows a low-magnification overview of the organoid IF, and the lower panel shows a magnified view of the yellow boxed areas in the upper panel: AQP5: Type I alveolar epithelium cells; TTF1 and SFTPC: Type II alveolar epithelium cells; SP-B: general lung tissue markers; Keratin 5 and P63: Basal cells; MUC5AC: Goblet cells; Foxj1: Ciliated cells. IF staining confirmed the presence of proximal airway epithelial cells positive for Keratin 5, P63 and MUC5AC, as well as distal alveolar epithelial cells positive for AQP5, TTF1 and SP-C, demonstrating the phenotypic fidelity of patient-derived lung organoids. **C** mRNA expression levels of lung cell-specific markers in hLOs assessed by RT-qPCR across three independent experiments, calculated using the $2^{-\Delta\Delta Ct}$ method, with GAPDH serving as the internal reference for normalization, and the background expression of undifferentiated hiPSCs used as the negative control (expression level set to 1). **D** IHC and H&E analysis of fibrotic hLOs. hLOs: Untreated human lung organoids; hLOF: hLOs co-cultured with human lung fibroblasts (HFs) at a 1:2 ratio; hLOF-F: hLOs co-cultured with human lung fibroblasts (HFs) at a 1:2 ratio and treated with 1μg/mL LPS and 25ng/mL TGF-β1 for 48-96 h, Scar bar: 50um. **E** RT-qPCR quantification of fibrotic marker expression (α-SMA, collagen I, fibronectin, and vimentin) in the fibrotic hLOs. **F Response of fibrotic hLOs** to anti-fibrotic drug treatment (nintedanib, 5 μM; pirfenidone, 40 μg/mL), RT-qPCR quantification of fibrotic marker expression (CTGF, α-SMA, collagen I, fibronectin, and vimentin). **G** Nintedanib-pirfenidone combination therapy in fibrotic hLOs: *Top:* the morphology changes (bright field); *Middle:* H&E staining; *Bottom:* α-SMA and Fibronectin IHC staining, Scar bar: 200um for BF; 50um for HE, a-SMA and Fibronectin. **H** RT-qPCR quantification of fibrotic marker expression for Nintedanib-pirfenidone combination therapy in fibrotic hLOs. The representative bright-field, immunofluorescence, H&E, and immunohistochemical images were obtained from one patient-derived hLO line and reproduced in three independently established organoid culture and modelling experiments. RT-qPCR data were obtained from hLO cultures independently established from three different patient samples, with each patient treated as one biological replicate (\(n=3\)). qPCR measurements were performed in technical triplicate, and technical replicate values were averaged before statistical analysis. All quantifications are shown as mean ± SEM. Statistical comparisons between two groups were performed using two-tailed unpaired Student's t-test. For comparisons among multiple groups, one-way analysis of variance (ANOVA) followed by Tukey's post hoc test. A p-value < 0.05 was considered statistically significant.

Figure 2 Macrophage Incorporation Modulates Fibrotic Responses in Human Lung

Organoid Co-Cultures. **A** The workflow for differentiating hiPSCs into macrophages. **B** Left panel: *Top:* Bright-field morphology of hiPSC-derived macrophages (hiMac). *Bottom:* Immunofluorescence staining confirming positive expression of the pan-macrophage marker CD68. Right panel: IF characterization of hiMac for the hematopoietic lineage marker CD45, the pan-macrophage marker CD68, and the M2-type macrophage marker CD163. The last column shows a magnified view of the yellow boxed areas in the first column. **C** Morphological feature of the fibrotic hLOs under bright-field and fluorescence imaging (hiMac shown in GFP). hLOF: hLOF coculture with HFs (1:2); hLOF-F: 1μg/mL LPS+25ng/mL TGF-β1 treated the coculture system of hLOs and HFs; hLOFM-F: 1μg/mL LPS+25ng/mL TGF-β1 treated the tri-culture system of hLO, HFs and hiMac. **D** Left: IF staining for α-SMA showing enhanced myofibroblast activation in the tri-culture human fibrotic model, Scale bars, 300 μm; Right: Quantitative analysis of the immunofluorescence (IF) images, showing the α-SMA fluorescence intensity and the percentage of α-SMA-positive area, which were normalized to DAPI intensity and DAPI positive areas respectively. **E** mRNA expression levels of fibrosis markers (Fibronectin, α-SMA, Vimentin and Collagen I,) assessed by RT-qPCR in the tri-culture model compared to hLOs and hLOF. The experiments were performed using hLOs derived from one patient. Three independently reconstructed co-culture experiments were conducted (n=3), with each experiment incorporating hiMacs generated from a separate independent hiPSC-to-macrophage differentiation batch. qPCR measurements were performed in technical triplicate, and technical replicate values were averaged before statistical analysis. All quantifications are presented as mean ± SEM. Statistical significance was determined by one-way and two-way analysis of variance (ANOVA) followed by Tukey's post hoc test. A p-value < 0.05 was considered statistically significant.

Figure 3 hiPSC-Derived Lung Organoids Express Multiple Pulmonary Epithelial-Associated Markers. **A** Schematic diagram and corresponding bright-field images illustrating the induction process and morphology of hiPSC-derived lung organoids (hiLOs) at key developmental stages. **B** Bright-field images demonstrate the capability of hiLOs for serial passaging, cryopreservation, and subsequent recovery without loss of core structural integrity. **C** IF analysis of hiLOs (Suspension culture) for key lung lineage markers of proximal (Keratin-5, MUC5AC) and distal (AQP5, TTF1) lung epithelial markers of hiLOs, Scale bars, 200 μm and 20 μm. **D** IF analysis of hiLOs (Suspension culture, P3) for key lung lineage markers of AQP5, Keratin-5, SFTPC and α-SMA showed retention of selected marker-positive populations after passaging, Scale bars, 100 μm and 20 μm. **E** RT-qPCR analysis validating the mRNA expression of characteristic lung tissue markers in d30-, P1- and P3-hiLOs (Suspension culture) compared to its undifferentiated hiPSCs (expression level set to 1). Data are from three independent hiPSC differentiation and co-culture experiments (n=3) which calculated by the ΔΔCt method, with GAPDH serving as the internal reference for normalization. All quantifications are presented as mean ± SEM. Statistical significance was determined by Student's t-test. A p-value < 0.05 was considered statistically significant.

Figure 4 Establishment of an iPSC-Based Lung Organoid–Fibroblast–Macrophage Tri-Culture Model. **A** Morphology of the tri-culture human lung fibrotic models under bright-

field and fluorescence microscopy (hiPSC-derived lung organoids (hiLOs) and hiMac shown in GFP). hiLOF: hiLOs co-culture with HFs (1:2); hiLOF-F: Co-culture of hiLOs and HFs treated with LPS (1µg/mL) + TGF-β1 (25 ng/mL); hiLOFM-F: Tri-culture system incorporating hiLOs, HFs, and hiMac under the same cytokine treatment. **B** IF staining for α-SMA demonstrating enhanced myofibroblast activation in the tri-culture pro-fibrotic niche, Scale bars, 1 mm; **C-D** Quantitative analysis of the immunofluorescence (IF) images, showing the α-SMA fluorescence intensity and the percentage of α-SMA-positive area, which were normalized to DAPI intensity and DAPI positive areas respectively. **E–F** RT-qPCR analysis of the fibrosis-associated markers (E) fibronectin and (F) vimentin and the inflammation-associated markers (G) IL-11 in the tri-culture fibrosis model compared to control and co-culture systems; **H** IL-1β concentrations in the culture medium**.** All data are from three independent hiPSC differentiation and co-culture experiments (n=3). All quantifications are presented as mean ± SEM. Statistical significance was determined by one-way analysis of variance (ANOVA) followed by Tukey's post hoc test. A p-value < 0.05 was considered statistically significant.

Figure 5 Bleomycin-induced fibrotic responses and their modulation by antifibrotic treatment in the hiPSC-derived tri-culture lung organoid model. **A–F** Fibrosis-, inflammation-, and alveolar epithelial lineage-associated responses of hiLOFM cultures exposed to the standard fibrosis-induction protocol (hiLOFM-F), bleomycin (BLM; 3 or 10 µg/mL), or the combination of TGF-β1 (25 ng/mL) with BLM (3 µg/mL). RT-qPCR analysis of (A) FN1, (B) COL1A1, (C) IL11, (E) AQP5, and (F) SFTPC expression. (D) IL-1β concentrations in the culture medium. **G–K** Pharmacological responses to combined treatment with nintedanib (5 µM) and pirfenidone (40 µg/mL) in hiLOFM-F cultures and TGF-β1 (25 ng/mL) with BLM (3 µg/mL) cultures. RT-qPCR analysis of (G) FN1, (H) IL11, (J) AQP5, and (K) SFTPC expression. (I) IL-1β concentrations in the culture medium. The standard hiLOFM-F induction protocol comprised LPS (1 µg/mL), TGF-β1 (25 ng/mL), as described in the Methods. Relative mRNA expression was calculated using the 2^−ΔΔCt method with hiLOs as the calibrator (hiLOs = 1). Unless otherwise indicated by horizontal connecting lines, P values displayed above individual bars represent comparisons with untreated hiLOFM. Data are presented as the mean ± SEM from three independent hiPSC differentiation and co-culture experiments (n=3). Statistical significance was determined using one-way ANOVA followed by Tukey's multiple-comparisons test. P < 0.05 was considered statistically significant.

Figure 6 The hiPSC-derived tri-culture lung organoid model detects DS-8201-associated epithelial, inflammatory, and profibrotic responses. **A** Representative immunofluorescence images of α-SMA (red), DAPI (blue), and the corresponding bright-field images of hiLOs, untreated hiLOFM, fibrosis-induced hiLOFM (hiLOFM-F), and hiLOFM treated with DS-8201 (5 µg/mL). Scale bars, 300 µm. **B–C** Quantification of the immunofluorescence images showing (B) the α-SMA-positive area normalized to the DAPI-positive area and (C) α-SMA fluorescence intensity normalized to DAPI fluorescence intensity. **D–G** and **I–K** RT-qPCR analysis of DS-8201-induced changes in (D) ACTA2, (E) FN1, (F) COL1A1, (G) IL11, (I) VIM, (J) AQP5, and (K) SFTPC expression following treatment with DS-8201 at 0.5, 5,

or 50 μg/mL. The hiLOFM-F group was generated using the standard fibrosis-induction protocol and served as a positive fibrotic control. **H** IL-1β concentrations in the culture medium following DS-8201 treatment. Relative mRNA expression was calculated using the 2^−ΔΔCt method with hiLOs as the calibrator (hiLOs = 1). Unless otherwise indicated by horizontal connecting lines, P values displayed above individual bars represent comparisons with untreated hiLOFM. Data are presented as the mean ± SEM from three independent hiPSC differentiation and co-culture experiments (n=3). Statistical significance was determined using one-way ANOVA followed by Tukey's multiple-comparisons test. $P < 0.05$ was considered statistically significant.

Figure 7 Schematic Overview of Model Development and Proof-of-Concept Pharmacological Assessment. We have developed and functionally validated a human LOs-HF-Mac tri-culture platform, the model incorporates lung epithelial, fibroblast and macrophage components and displays selected inflammatory and fibrotic-associated responses following LPS/TGF-β1 exposure. Responses to established antifibrotic agents support its potential use in preliminary pharmacological assessment, while its detection of DS-8201-associated responses highlights its potential utility in the early-stage evaluation of drug-associated pulmonary effects.

Figure S1 Identification the cell markers and passaging stability of the Mouse Lung Organoids. mLOs were derived from endogenous epithelial stem/progenitor cells of mouse lung tissues. **A** IF staining validating key pulmonary cell identities in mLOs, including: Epcam: epithelium cells; AQP5: Type I alveolar epithelium cells; TTF1: Lung epithelium cells; P63: Basal cells; MUC5AC: Goblet cells. The right column shows a magnified view of the yellow boxed areas in the first column. Aqp5-positive AT1 cells with the typical elongated, flattened morphology shown in yellow arrow. **B** Representative bright-field images showing the morphology of mLOs during multiple passages (P1-P4) and post-thaw (P5, P6). All data are from three independent hiPSC differentiation and co-culture experiments (n=3).

Figure S2 Establishment and Pharmacological Characterization of a Mouse Lung Organoid Model Displaying Fibrosis-Associated Features. Mouse lung organoids (mLOs) were derived from endogenous epithelial stem/progenitor cells of mouse lung tissues. **A** Representative bright-field images showing the morphology of mLOs during culture (**a-b**: solid organoids; **c-d**: cystic organoids). **B** Schematic or representative images of fibroblast sources used in this study, including mouse embryonic fibroblasts (MEF), commercial human embryonic lung fibroblasts (HFL-1), and human lung tumor-derived fibroblasts (samples 0619 and 0457). **C** Morphological comparison of organoids under different culture conditions: mLOs: Untreated lung organoids; mLOs-F: Lung organoids treated with 1μg/mL LPS and 25 ng/mL TGF-β1; mLOF: Lung organoids co-cultured with MEFs at a 1:2 ratio.; mLOF-F: Co-culture system treated with 1μg/mL LPS and 25 ng/mL TGF-β1. **D** Histological analysis of fibrotic organoids by hematoxylin and eosin (H&E) staining and immunohistochemistry (IHC) for key fibrosis markers: Collagen I, Fibronectin, and α-smooth muscle actin (α-SMA). **E** mRNA expression levels of α-SMA and Collagen I

assessed by RT-qPCR across the indicated conditions. **F** Evaluation of anti-fibrotic drug responses in the fibrosis model: *Top:* Bright-field morphology of organoids treated with nintedanib (5 μM) or pirfenidone (20 μg/mL); *Bottom:* IHC staining for α-SMA following drug treatment. **G** RT-qPCR analysis of fibrosis-related genes (α-SMA, Collagen I and MMP2) in organoids after treatment with nintedanib or pirfenidone. All data are from three independent hiPSC differentiation and co-culture experiments (n=3). All quantitative results are presented as mean ± SEM. Statistical significance was determined by one-way analysis of variance (ANOVA) followed by Tukey's post hoc test. A p-value < 0.05 was considered statistically significant.

Figure S3 Mouse pulmonary fibrosis model establishment and validation. **A** Morphological comparison of organoids embedded in Matrigel: mLOs: Untreated mouse lung organoids embedded in Matrigel; mLOs-F: mLOs embedded in Matrigel and treated with 1μg/mL LPS and 25 ng/mL TGF-β1; mLOF-F: Co-culture system embedded in Matrigel and treated with 1μg/mL LPS and 25 ng/mL TGF-β1. **B** mRNA expression levels of α-SMA and Collagen I assessed by RT-qPCR across the indicated conditions. **C-D** Nintedanib-pirfenidone combination therapy in mLOF-F model. C: the morphology changes (bright field); D: mRNA expression levels of α-SMA and Collagen I assessed by RT-qPCR across. All quantifications are presented as mean ± SEM. All data are from three independent hiPSC differentiation and co-culture experiments (n=3). Statistical significance was determined by one-way analysis of variance (ANOVA) followed by Tukey's post hoc test. A p-value < 0.05 was considered statistically significant.

Figure S4 Human pulmonary fibrosis model establishment and validation. **A** Histological analysis of fibrotic organoids by BF, H&E staining and IHC for key fibrosis markers: Collagen I, Fibronectin, and α-SMA. **B** mRNA expression levels of α-SMA, Collagen I, Fibronectin and Vimentin assessed by RT-qPCR across the indicated conditions. hLOs-F: 1μg/mL LPS and 25ng/mL TGF-β1 treated hLOs for 48-96 h. All quantifications are presented as mean ± SEM. All data are from three independent hiPSC differentiation and co-culture experiments (n=3). Statistical significance was determined by Student's t-test. A p-value < 0.05 was considered statistically significant. **C** Representative bright-field images of hLOs established from three different lung cancer patients (2128, 0217, 0814). up: control hLOs; hLOF-F: hLOs coculture with its HF and stimulated with LPS+TGF-β1.

Figure S5 Morphological and Passaging Stability Characterization of hiLOs. **A** IF staining validating cell identities in hiLOs, including: Epcam: epithelium cells; MUC5AC: Goblet cells. Data are representative of three independent differentiations. The right column shows a magnified view of the yellow boxed areas in the first column. **B** Bright-field images of hiLOs at different passages (D30, D50, P1, P3), post-thaw (P4, P5). **C** The proportion of AQP5+, α-SMA+, Keratin-5+ and SFTPC+ cells estimated based on the IF images of P1- and P3-hiLOs. The data describe the relative abundance of these marker-positive populations across the passages examined. All quantifications are presented as mean ± SEM. All data are from three independent hiPSC differentiation and co-culture experiments (n=3). Statistical significance was determined by one-way analysis of variance (ANOVA) followed

by Tukey's post hoc test. A p-value < 0.05 was considered statistically significant.

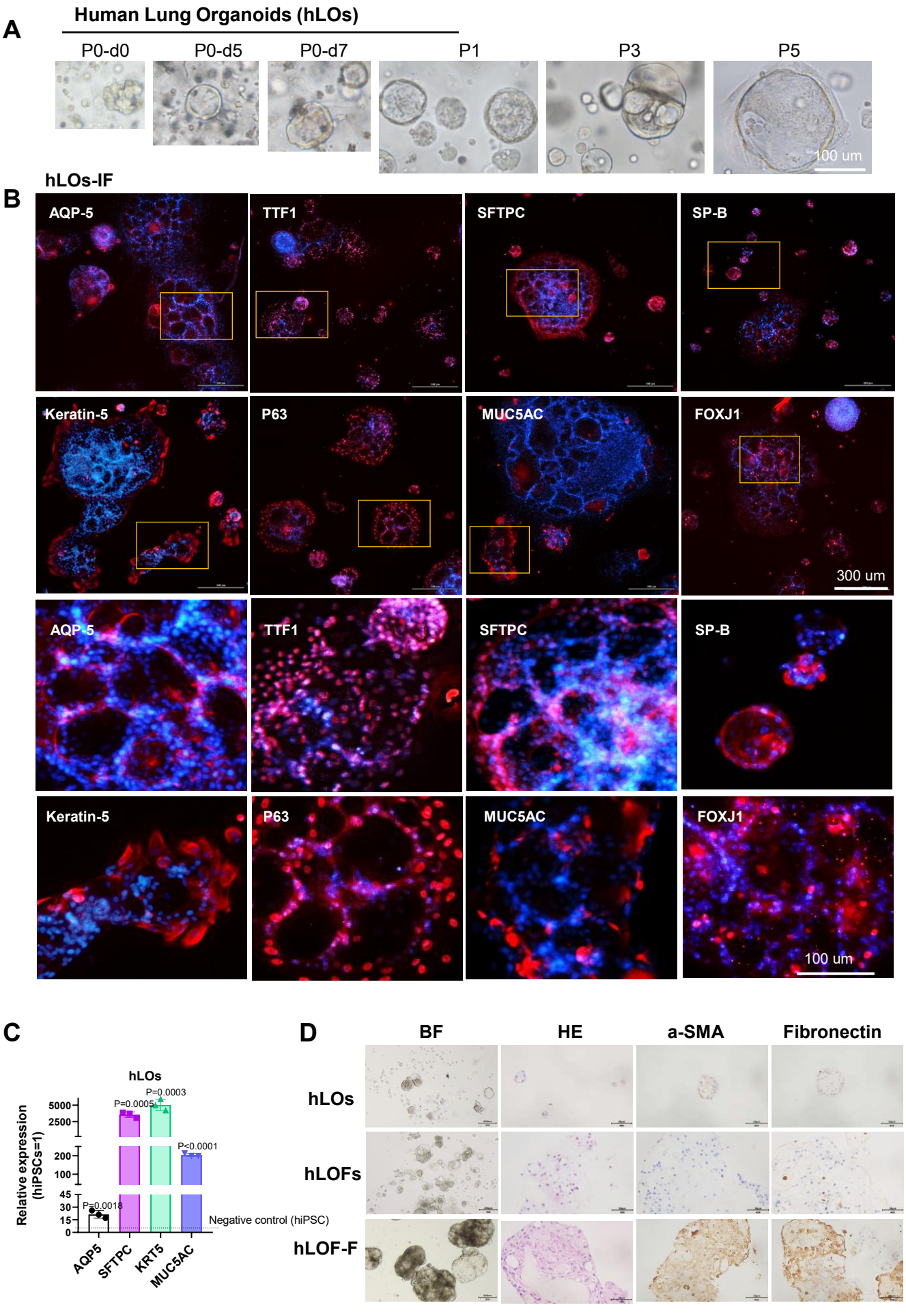
Figure S6 Passaged Lung Organoids Support Reconstruction of the Pulmonary Fibrosis Model. **A** Morphology of organoids under different culture conditions: hiLOF constructed using P3 hiLOs; hiLOF-F: hiLOs of P3 cocultured with HF and treated with 1μg/mL LPS and 25 ng/mL TGF-β1; hiLOM-F: hiLOs of P3 cocultured with hiMacro and treated with 1μg/mL LPS and 25 ng/mL TGF-β1; hiLOFM: hiLOs of P3 cocultured with HF and hiMacro. hiLOFM-F: hiLOs of P3 cocultured with HF and hiMacro and treated with 1μg/mL LPS and 25 ng/mL TGF-β1; **B-C** RT-qPCR analysis of fibrosis markers (B) α-SMA, Fibronectin, Vimentin and Collagen I; and inflammation marker (C) IL-6, IL-1β and IL8 in the two- and tri-culture model following induction of fibrosis using: 1μg/mL LPS+25ng/mL TGF-β1. The data indicate that P3 hiLOs retained the capacity to support reconstruction of the fibrosis model. All quantifications are presented as mean ± SEM. All data are from three independent hiPSC differentiation and co-culture experiments (n=3). Statistical significance was determined by one-way analysis of variance (ANOVA) followed by Tukey's post hoc test. A p-value < 0.05 was considered statistically significant.

Suppl.Video1-4 Videos of the processes for cells aggregation in hLOs, hLOF, hLOF-F and hLOFM-F.

Suppl.Video5.1-5.2 Videos of the hiLOs exhibited spontaneous rhythmic contractions.

Suppl.Video6-9 Videos of the processes for cells aggregation in hiLOs, hiLOF, hiLOF-F and hiLOFM-F.

All supplementary videos are openly available in Zenodo at https://doi.org/10.5281/zenodo.21502299.


A
Human Lung Organoids (hLOs)
P0-d0
P0-d5
P0-d7
P1
P3
P5
100 um
B
hLOs-IF
AQP-5
TTF1
SFTPC
SP-B
Keratin-5
P63
MUC5AC
FOXJ1
300 um
AQP-5
TTF1
SFTPC
SP-B
Keratin-5
P63
MUC5AC
FOXJ1
100 um
C
hLOs
Relative expression (hiPSCs=1)
5000
2500
200
100
45
30
15
0
P=0.0003
P=0.0005
P<0.0001
P=0.0018
Negative control (hiPSC)
AQP5
SFTPC
KRT5
MUC5AC
D
BF
HE
a-SMA
Fibronectin
hLOs
hLOFs
hLOF-F

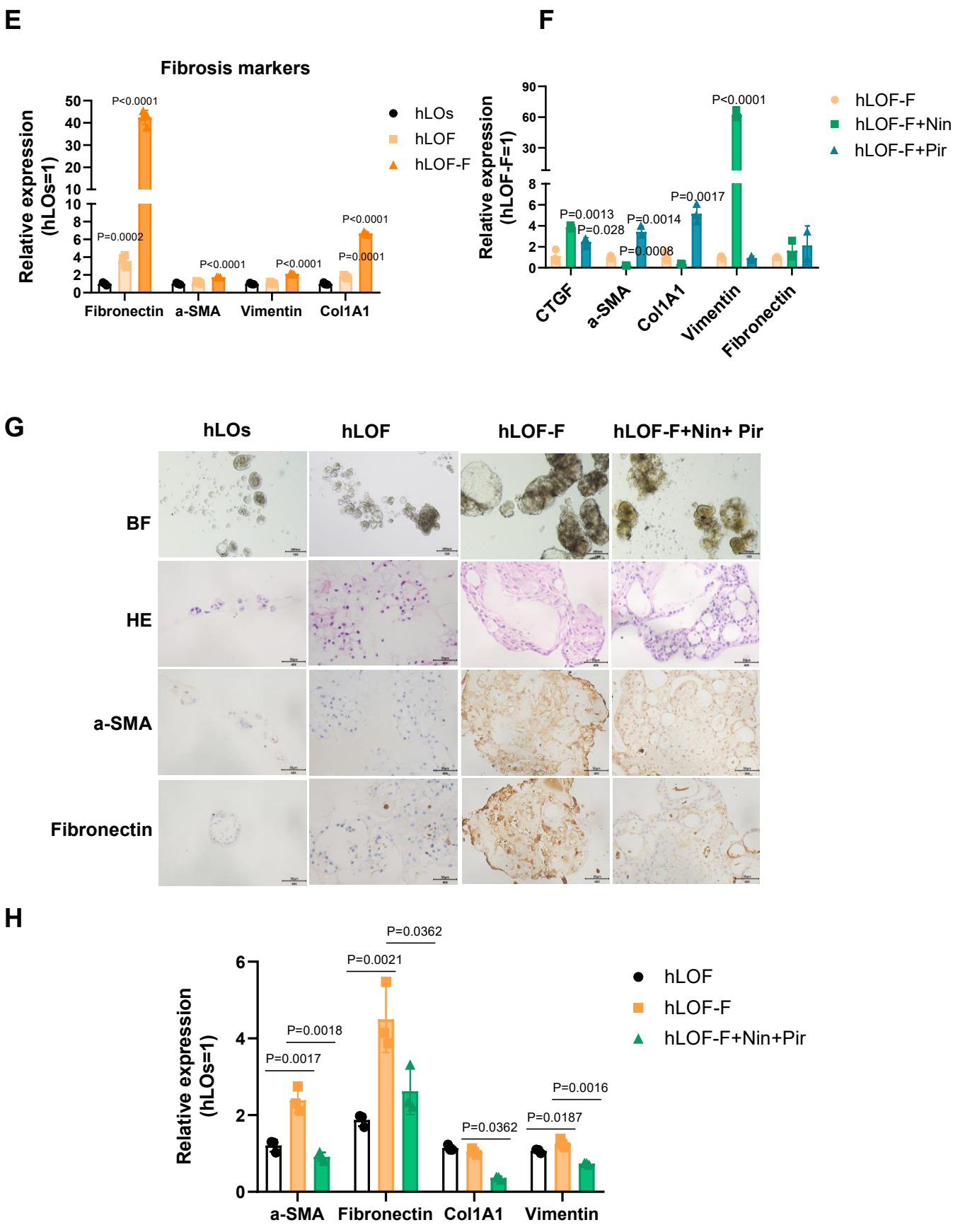
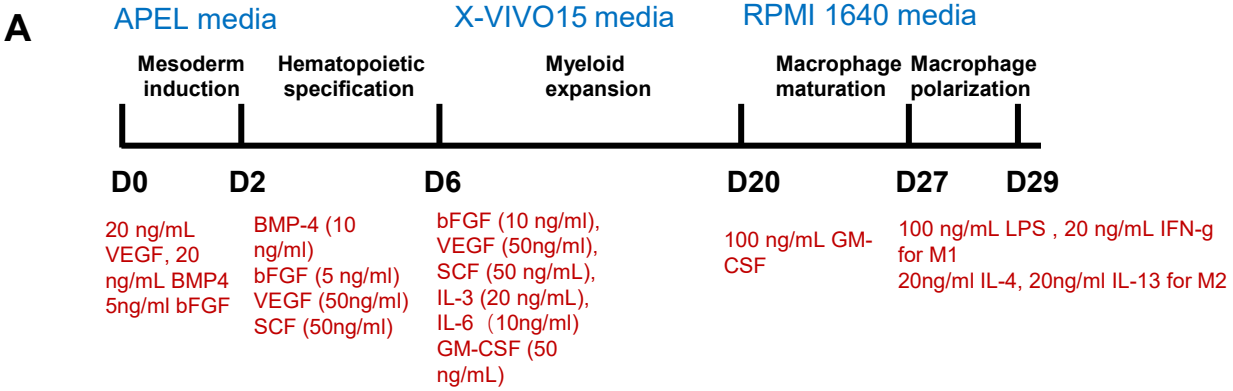
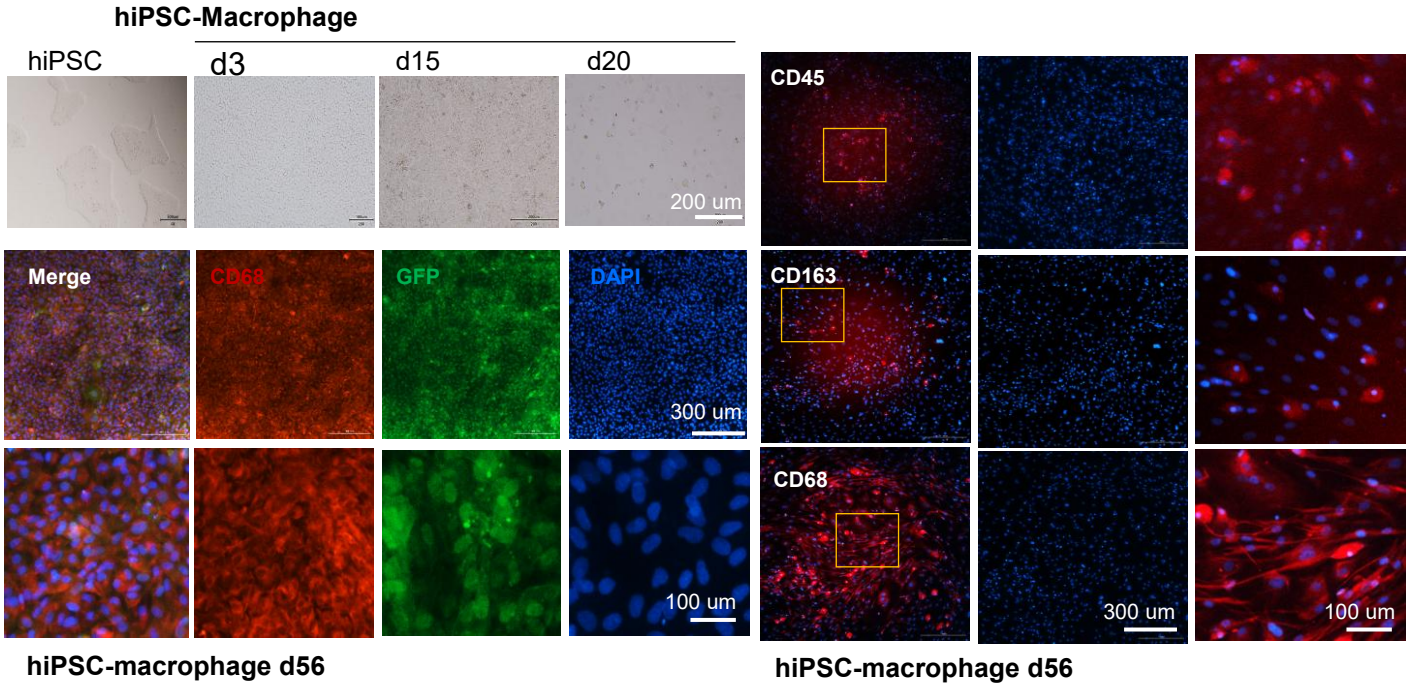


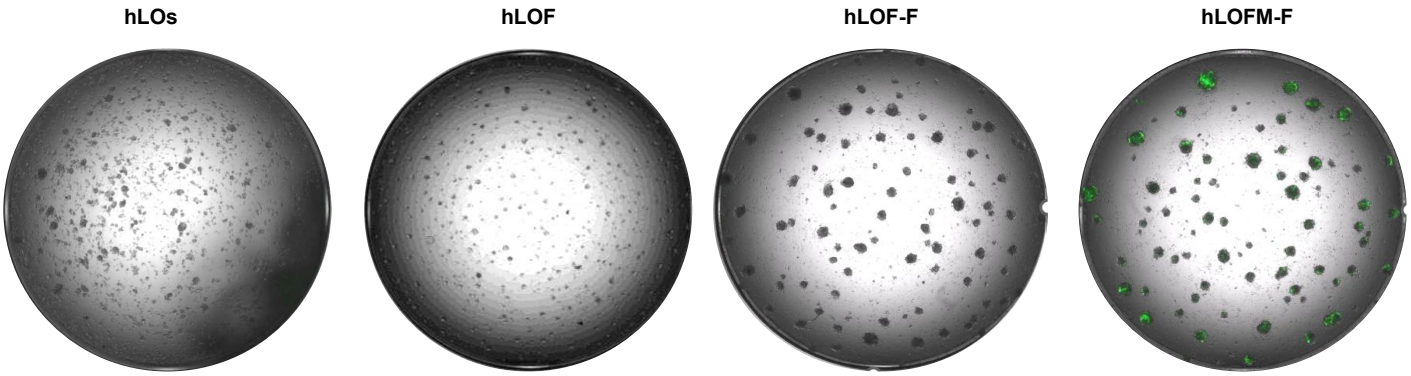
Figure 1 A Primary Human Lung Organoid Co-Culture Model Displaying Fibrosis-Associated Drug Responses


A
APEL media
X-VIVO15 media
RPMI 1640 media
Mesoderm induction
Hematopoietic specification
Myeloid expansion
Macrophage maturation
Macrophage polarization
D0
D2
D6
D20
D27
D29
20 ng/mL VEGF, 20 ng/mL BMP4 5ng/ml bFGF
BMP-4 (10 ng/ml) bFGF (5 ng/ml) VEGF (50ng/ml) SCF (50ng/ml)
bFGF (10 ng/ml), VEGF (50ng/ml), SCF (50 ng/mL), IL-3 (20 ng/mL), IL-6 (10ng/ml) GM-CSF (50 ng/mL)
100 ng/mL GM-CSF
100 ng/mL LPS , 20 ng/mL IFN-g for M1
20ng/ml IL-4, 20ng/ml IL-13 for M2

B


hiPSC-Macrophage
hiPSC
d3
d15
d20
200 um
Merge
CD68
GFP
DAPI
300 um
100 um
hiPSC-macrophage d56
CD45
CD163
CD68
300 um
100 um
hiPSC-macrophage d56

C


hLOs
hLOF
hLOF-F
hLOFM-F

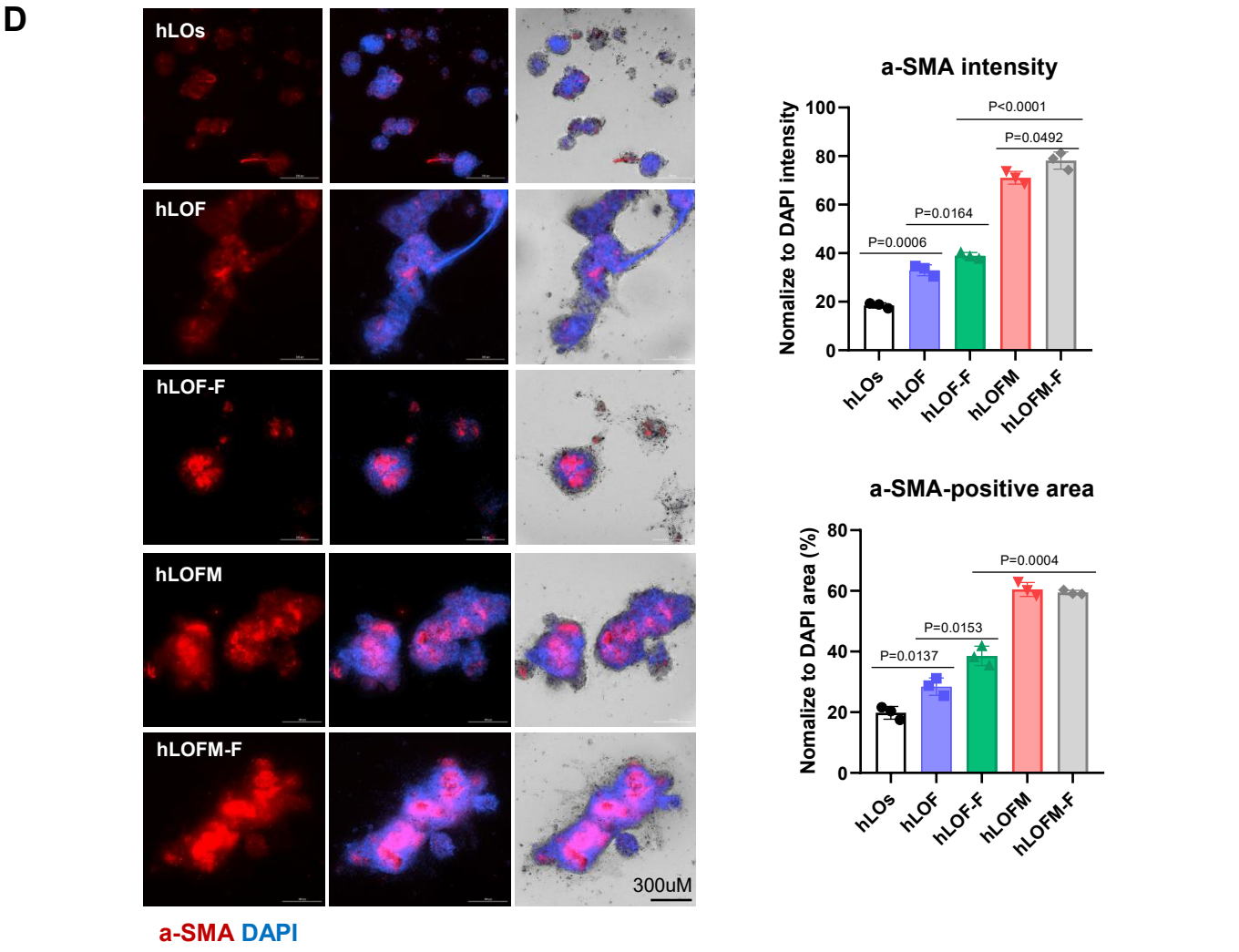
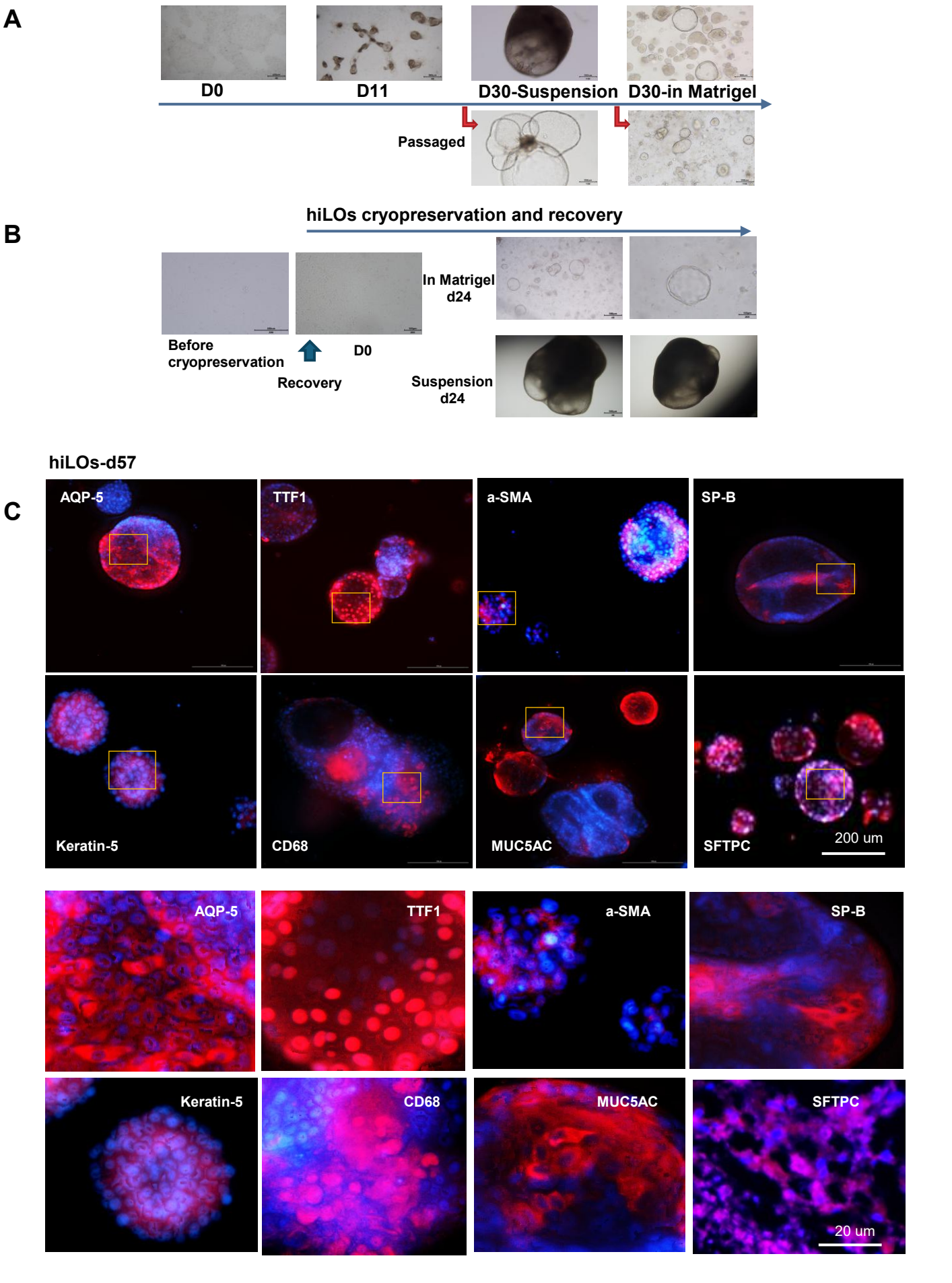
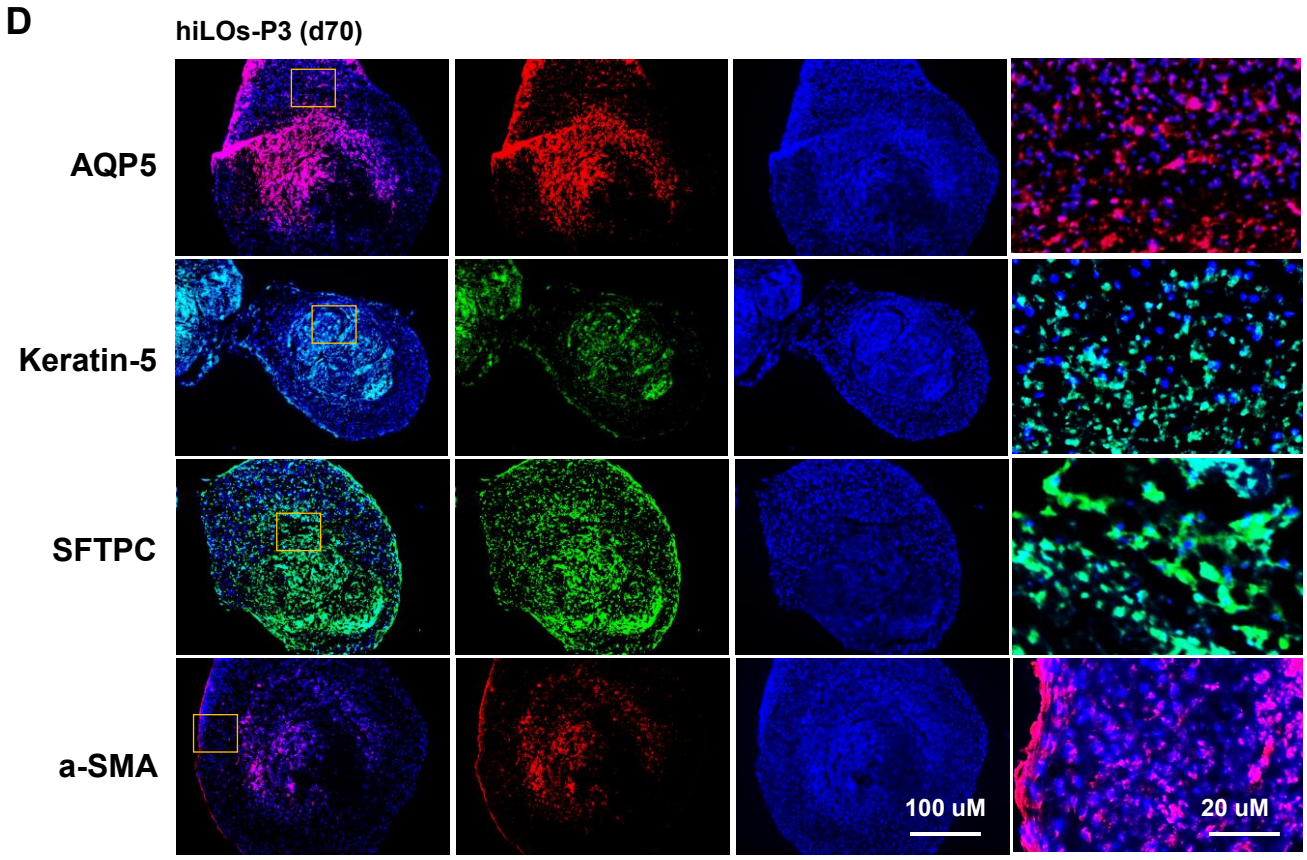


Figure 2 Macrophage Incorporation Modulates Fibrotic Responses in Human Lung Organoid Co-Cultures


A
D0
D11
D30-Suspension
D30-in Matrigel
Passaged
B
hiLOs cryopreservation and recovery
In Matrigel d24
Before cryopreservation
D0
Recovery
Suspension d24
hiLOs-d57
C
AQP-5
TTF1
a-SMA
SP-B
Keratin-5
CD68
MUC5AC
SFTPC
200 um
AQP-5
TTF1
a-SMA
SP-B
Keratin-5
CD68
MUC5AC
SFTPC
20 um



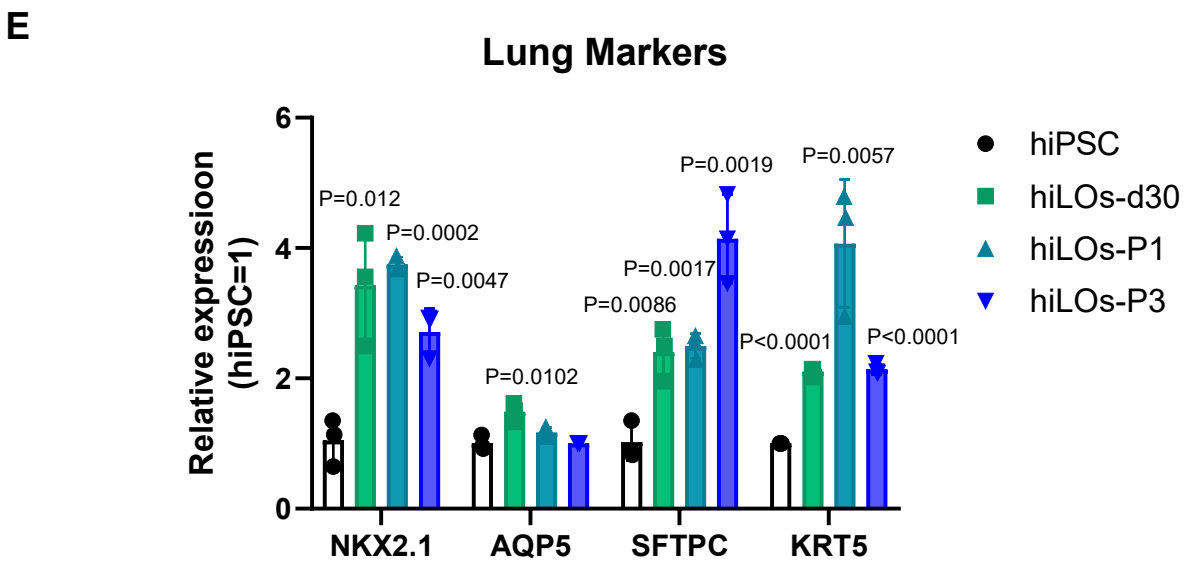


Figure 3 hiPSC-Derived Lung Organoids Express Multiple Pulmonary Epithelial-Associated Markers

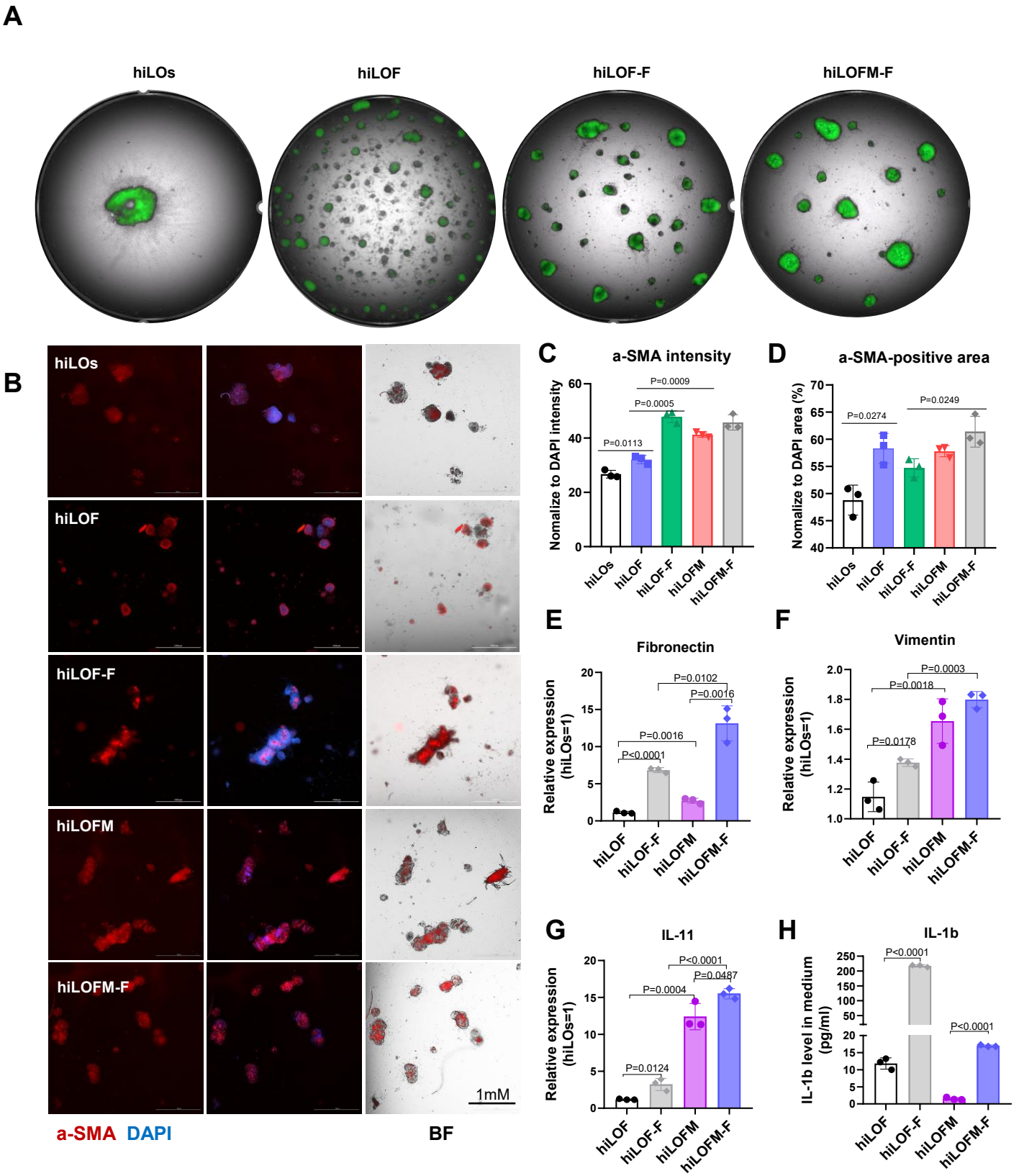


Figure 4 Establishment of an iPSC-Based Lung Organoid–Fibroblast–Macrophage Tri-Culture Model

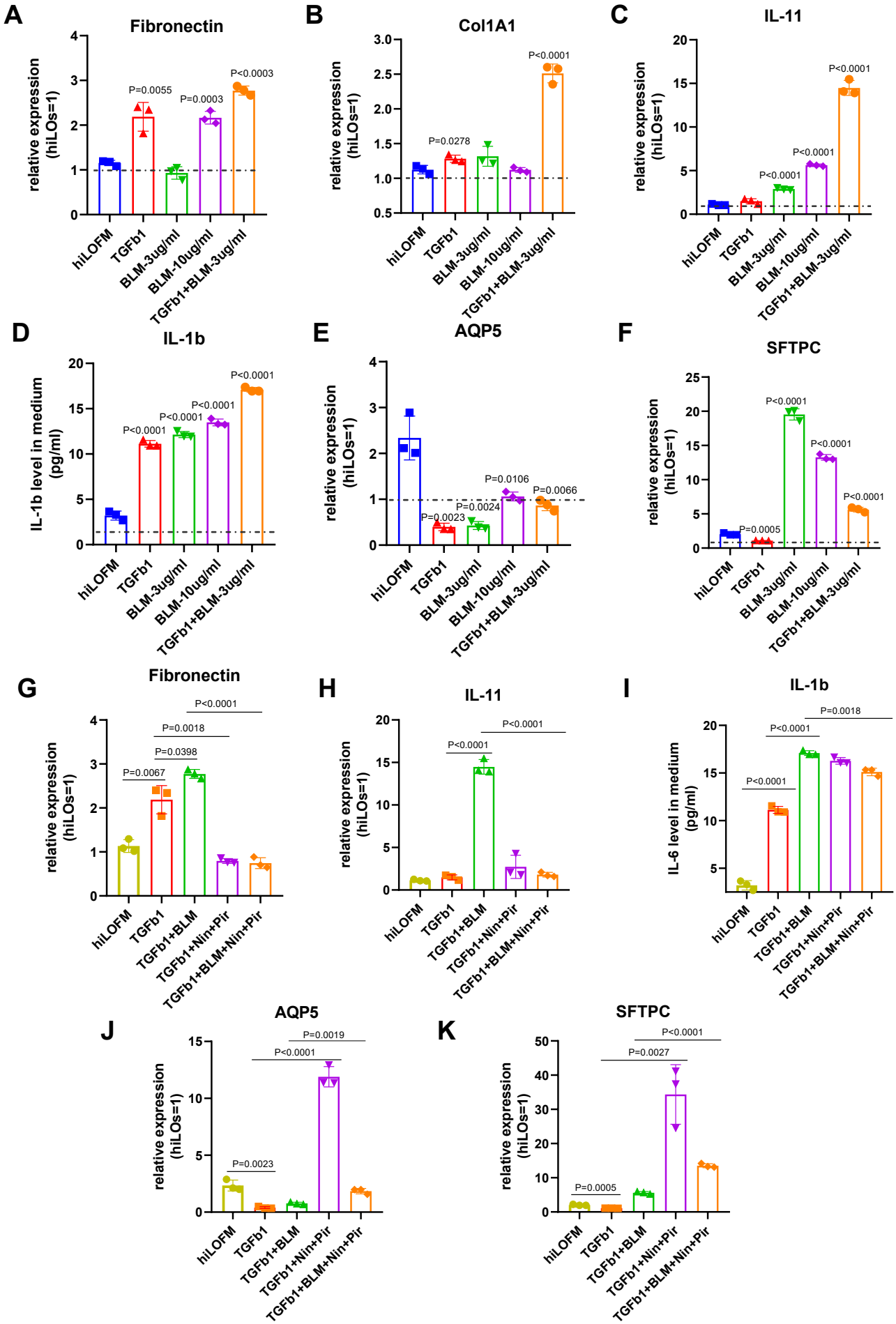


Figure 5 Bleomycin-induced fibrotic responses and their modulation by antifibrotic treatment in the hiPSC-derived tri-culture lung organoid model

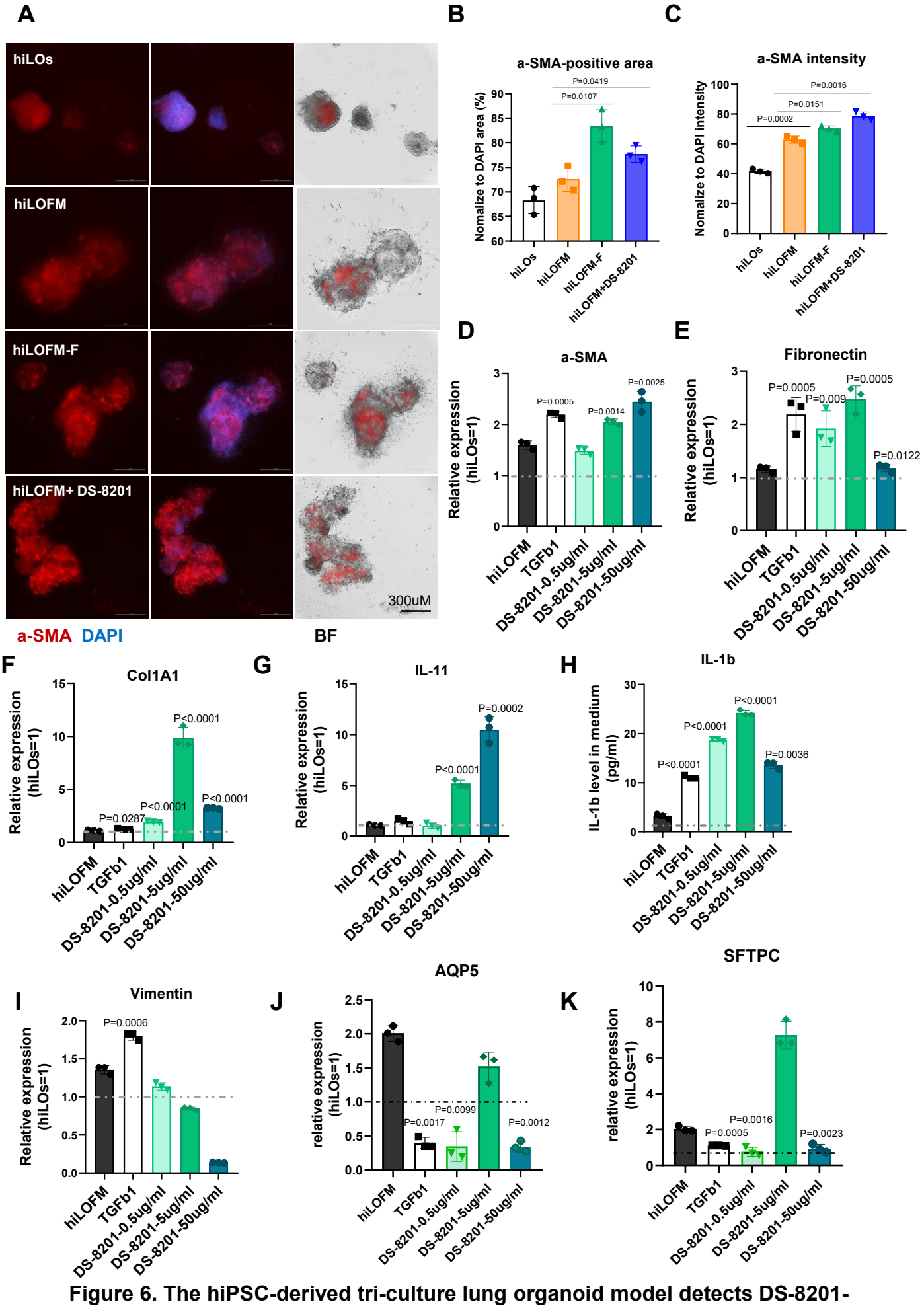


Figure 6. The hiPSC-derived tri-culture lung organoid model detects DS-8201-associated epithelial, inflammatory, and profibrotic responses

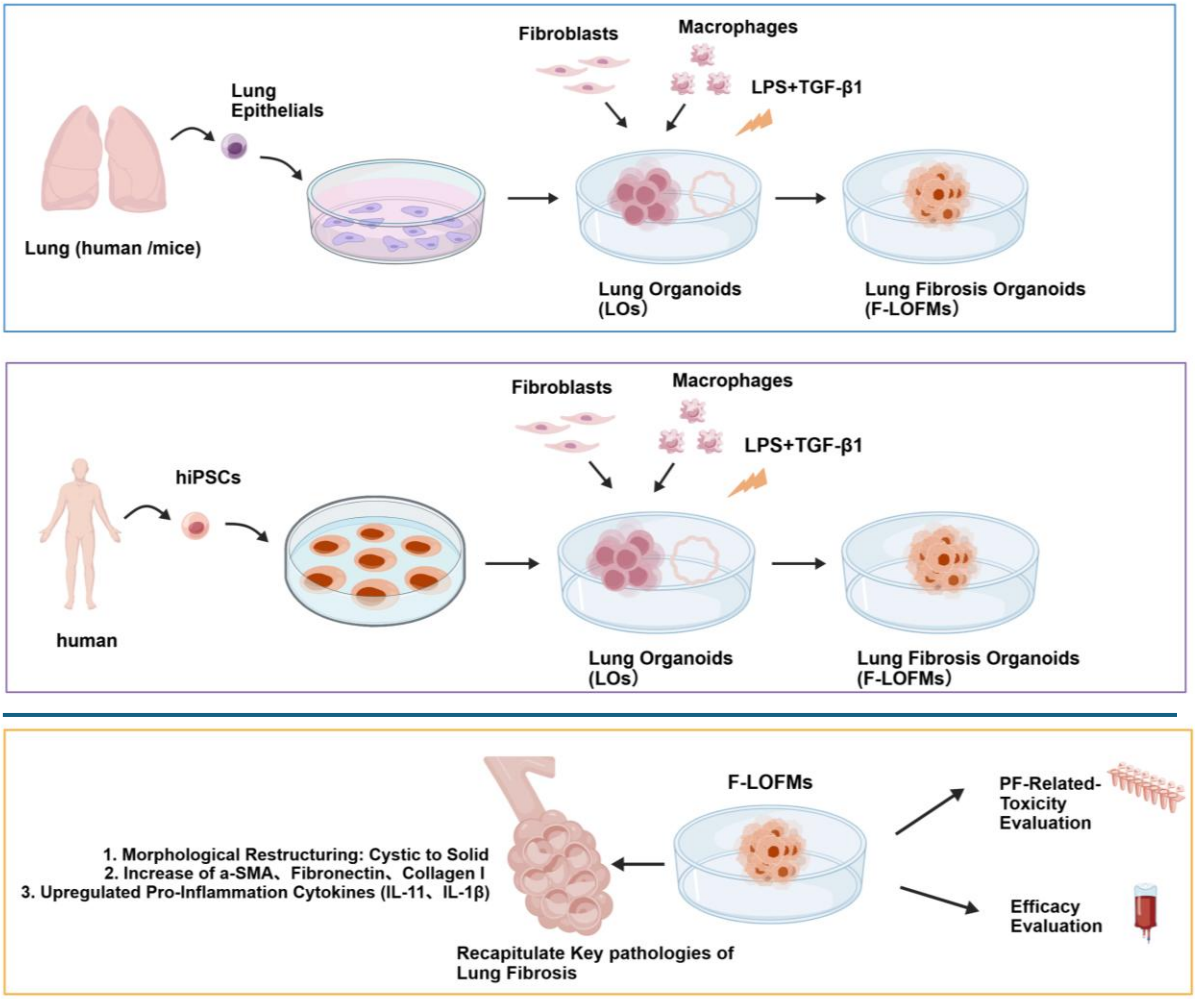


Figure 7 Schematic Overview of Model Development and Proof-of-Concept Pharmacological Assessment. We have developed and functionally validated a human LOs-HF-Mac tri-culture platform, the model incorporates lung epithelial, fibroblast and macrophage components and displays selected inflammatory and fibrotic-associated responses following LPS/TGF-β1 exposure. Responses to established antifibrotic agents support its potential use in preliminary pharmacological assessment, while its detection of DS-8201-associated responses highlights its potential utility in the early-stage evaluation of drug-associated pulmonary effects.

Supplementary Files

This is a list of supplementary files associated with this preprint. Click to download.

- supplementaryfigure.pdf
- Supplementarymaterials.docx